






Plant defense compound triggers mycotoxin synthesis by regulating H2B ub1 and H3K4 me2/3 deposition

Tianling Ma¹ , Lixin Zhang¹, Minhui Wang¹, Yiqing Li¹, Yunqing Jian¹, Liang Wu² , Harold Corby Kistler³ , Zhonghua Ma¹  and Yanni Yin¹ 

¹State Key Laboratory of Rice Biology, Institute of Biotechnology, Zhejiang University, 866 Yuhangtang Road, Hangzhou 310058, China; ²Institute of Crop Science, Zhejiang University, 866 Yuhangtang Road, Hangzhou 310058, China; ³United States Department of Agriculture, Agricultural Research Service, 1551 Lindig Street, St Paul, MN 55108, USA

Summary

- *Fusarium graminearum* produces the mycotoxin deoxynivalenol (DON) which promotes its expansion during infection on its plant host wheat. Conditional expression of DON production during infection is poorly characterized.
- Wheat produces the defense compound putrescine, which induces hypertranscription of DON biosynthetic genes (*FgTRIs*) and subsequently leads to DON accumulation during infection. Further, the regulatory mechanisms of *FgTRIs* hypertranscription upon putrescine treatment were investigated.
- The transcription factor FgAreA regulates putrescine-mediated transcription of *FgTRIs* by facilitating the enrichment of histone H2B monoubiquitination (H2B ub1) and histone 3 lysine 4 di- and trimethylations (H3K4 me2/3) on *FgTRIs*. Importantly, a DNA-binding domain (bZIP) specifically within the *Fusarium* H2B ub1 E3 ligase Bre1 orthologs is identified, and the binding of this bZIP domain to *FgTRIs* depends on FgAreA-mediated chromatin rearrangement. Interestingly, H2B ub1 regulates H3K4 me2/3 via the methyltransferase complex COMPASS component FgBre2, which is different from *Saccharomyces cerevisiae*.
- Taken together, our findings reveal the molecular mechanisms by which host-generated putrescine induces DON production during *F. graminearum* infection. Our results also provide a novel insight into the role of putrescine during phytopathogen–host interactions and broaden our knowledge of H2B ub1 biogenesis and crosstalk between H2B ub1 and H3K4 me2/3 in eukaryotes.

Author for correspondence:
Yanni Yin
Email: ynyin@zju.edu.cn

Received: 3 June 2021
Accepted: 30 August 2021

New Phytologist (2021) 232: 2106–2123
doi: 10.1111/nph.17718

Key words: deoxynivalenol (DON), epigenetic regulation, *Fusarium graminearum*, phytopathogen–host interactions, plant defense compound.

Introduction

The plant pathogen *Fusarium graminearum* causes Fusarium head blight (FHB) on wheat, barley, maize and other important cereal crops (Goswami & Kistler, 2004). Fusarium head blight is a devastating disease and results in substantial yield losses as well as serious mycotoxin contamination (Pestka, 2010). One of these contaminants, the type B trichothecene, deoxynivalenol (DON), is the most frequently detected mycotoxin in cereal grains worldwide, with a 59% average incidence rate (Lee & Ryu, 2017). Deoxynivalenol impedes protein synthesis via binding to the ribosome, and in mammals causes vomiting, anorexia, immune dysregulation, growth and reproductive defects, and teratogenic effects (Pestka, 2010). In the last two decades, DON contamination of food and feed has become a challenging social issue as a result of the increased frequency and severity of FHB epidemics worldwide as well as the high toxicity of DON (Liu *et al.*, 2016; Chen *et al.*, 2019).

Given the importance of DON as a health threat, its biosynthetic pathway and environmentally mediated regulatory mechanisms have been extensively investigated. Deoxynivalenol

biosynthesis results from 15 trichothecene genes (*TRIs*), which are distributed at a 12-gene core *TRI* cluster, the *TRI1-TRI16* locus, and the single-gene *TRI101* locus in *F. graminearum* (Alexander *et al.*, 2009). Acidic pH has been reported to promote *FgTRIs* expression and DON production (Merhej *et al.*, 2010), while the pH regulatory factor FgPac1 is responsible for DON biosynthesis inhibition under alkaline pH (Jawad *et al.*, 2011a). Light affects DON production through the fungal-specific regulator velvet complex VelB/VeA/LaeA in *F. graminearum* (Merhej *et al.*, 2012; Kim *et al.*, 2013). Carbon sources sucrose, 1-kestose, and nystose, as well as secondary nitrogen source polyamines can stimulate DON production (Feng *et al.*, 2008; Gardiner *et al.*, 2009).

Besides its direct biological toxicity, DON has also been reported to be an important virulence factor for *F. graminearum*, playing a critical role in the spread of the pathogen within host tissues (Bai *et al.*, 2002; Carin *et al.*, 2005; Stephens *et al.*, 2008; Ilgen *et al.*, 2009; Bonnighausen *et al.*, 2019). Importantly, *F. graminearum* can produce enormous amounts of DON during infection on wheat heads, whereas little is produced during vegetative growth (Voigt *et al.*, 2005; Mudge *et al.*, 2006; Kazan *et al.*,

2012; Bonnighausen *et al.*, 2019). Evidently, there is a complex spectrum of regulatory signals for DON induction during infection. Recent studies have found that several host-generated compounds, H_2O_2 , 1-kestose, ferulic acid, coumaric acid, and polyamines, are induced during infection. These compounds have been reported to regulate DON biosynthesis *in vitro* (Ponts *et al.*, 2007; Gardiner *et al.*, 2009; Nadia *et al.*, 2011; Kazan *et al.*, 2012). However, the evidence that these compounds induce DON production during infection and the corresponding mechanisms by which they trigger DON accumulation are mostly lacking.

In eukaryotes, epigenetic regulation plays a vital role in rapid response to external stresses and orchestrating secondary metabolite biosynthesis (Macheleidt *et al.*, 2016; Dubey & Jeon, 2017). Our previous study showed the methyltransferase FgSet1 regulates the enrichment of histone 3 lysine 4 di- and trimethylation (H3K4 me2/3) on *FgTRs*, further promoting *FgTRs* transcription and DON production (Liu *et al.*, 2015). In *Drosophila*, budding yeast and humans, H2B monoubiquitination (H2B ub1) has been reported to be a prerequisite of H3K4 me2/3 (Kim *et al.*, 2009; Chandrasekharan *et al.*, 2010; Shilatifard, 2012). H2B ub1 is catalyzed by ubiquitin-conjugating enzyme (E2) Rad6 and ligase (E3) Bre1, which are highly conserved in eukaryotes (Fuchs & Oren, 2014). This chromatin mark is associated with transcriptional regulation of specific genes rather than the whole genome (Segala *et al.*, 2016). However, how H2B ub1 is induced and precisely enriched to the target chromosome is poorly understood (Gallego *et al.*, 2016). Moreover the molecular events of H2B ub1 regulating H3K4 me2/3 remain unclear and controversial in eukaryotes (Jeon *et al.*, 2018; Hsu *et al.*, 2019; Bae *et al.*, 2020). Therefore, we were interested in determining whether H2B ub1 and H3K4 me2/3 synergistically modulate DON biosynthesis, and in exploring the biogenesis mechanisms of these two histone modifications.

As an adaptation to environmental stimuli and pathogen attack, plants usually generate the secondary nitrogen source polyamines to help them survive (Walters, 2003; Bonnighausen *et al.*, 2019). Putrescine, spermidine and spermine are the major forms of polyamines (Haggag & Abd-El-Kareem, 2009; Matam & Parvatam, 2017). Here, we found that only putrescine can promote *FgTRs* transcription and DON production during *F. graminearum* infection. Further, our study revealed that the fungal secondary nitrogen source utilization regulator FgAreA modulated putrescine-induced DON production by enhancing enrichment of H2B ub1 and H3K4 me2/3 on *FgTRs*. In addition, we elucidated the biogenesis of H2B ub1 on *FgTRs* regulated by FgAreA upon putrescine induction, and the molecular events between H2B ub1 and H3K4 me2/3 in *FgTRs* transcriptional regulation. Overall, our study reveals the mechanisms by which the host defense compound putrescine promotes DON production in *F. graminearum* during infection. The results of this study will provide novel insights into the role of host defense compounds during phytopathogen–host interactions and advance the knowledge of H2B ub1 and H3K4 me2/3 biogenesis in eukaryotic organisms.

Materials and Methods

Fungal strains and phenotype determination

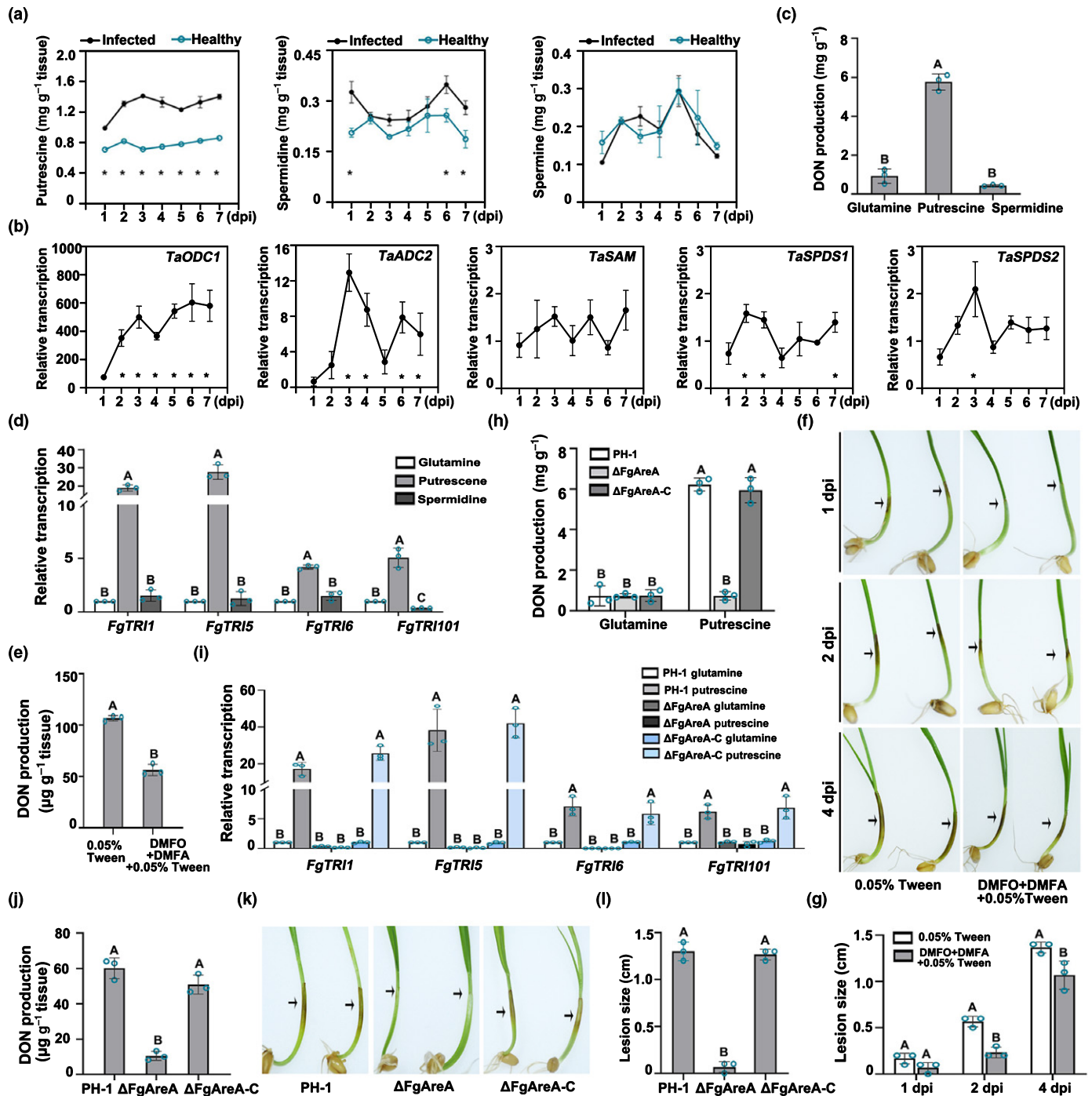
The wild-type strain PH-1 (NRRL 31084) of *F. graminearum* was used as a parental strain for transformation experiments. Mycelial growth of PH-1 and the resulting transformants were assayed on potato dextrose agar (PDA), as described previously (Yun *et al.*, 2015). Methods for determining stress sensitivity, virulence and DON production are presented in Supporting Information Methods S1.

For plant polyamine quantification, a 10 μ l aliquot of *F. graminearum* conidial suspension (10^5 ml⁻¹) was injected into all of the florets on the wheat head at anthesis. Sterile distilled water was inoculated in same way as the control. The inoculated wheat heads were sampled every day during the first 7 d post-inoculation (dpi) and diseased spikelets were collected for polyamine quantification. The quantification of polyamine in infected and noninfected wheat heads was performed by Provincial Key Laboratory of Agrobiolgy, Institute of Food Crops, Jiangsu Academy of Agricultural Sciences (Nanjing, China) using ultra performance liquid chromatography tandem mass spectrometry (UPLC-MS/MS). Briefly, plant material was ground in liquid nitrogen with a mortar and pestle, then 0.5 g powder was extracted in 10 ml of 90% acetonitrile and 2% formic acid. After centrifugation, the supernatant was collected, and pellet plant material was used for the second extraction in the same buffer. Subsequently, the supernatant collected from two rounds was filtrated through a 0.22 μ m organic filter and then injected onto a UPLC-MS/MS apparatus (Shimadzu 30A LC system; Kyoto, Japan) with a Triple Quad 6500 plus (Sciex; Redwood City, CA, USA).

To assess the effect of putrescine biosynthesis inhibitors on virulence and DON production, the surface of wheat seeds was disinfected with 2% sodium hypochlorite for 10 min, rinsed in several changes of sterile distilled water and then imbibed in 2 mM putrescine biosynthesis inhibitor DL- α -difluoromethylarginine (DFMA) and 2 mM putrescine biosynthesis inhibitor DL- α -difluoromethylornithine (DFMO) with 0.05% (v/v) Tween 20 (pH 7.0) or Tween 20 only (control) for 24 h before aseptic germination. Then 3-d-old coleoptiles were used for later virulence assays and DON production determination as described earlier.

Chromatin immunoprecipitation-qPCR analyses

Chromatin immunoprecipitation (ChIP) was performed based on the published protocol with additional modifications (Kaufmann *et al.*, 2010). Briefly, fresh mycelia of each sample were cross-linked with 1% formaldehyde for 10 min and then the reaction was stopped with 125 mM glycine for 5 min. Subsequently, samples were grounded in liquid nitrogen and suspended in lysis buffer with protease inhibitor (Sangon, Shanghai, China). DNA was sheared into 200–500 bp fragments with 30 s on and 30 s off in a Bioruptor Plus (Diagenod UCD-300; Liège, Belgium). After centrifugation, the supernatant was diluted with 10 \times ChIP



dilution buffer (1.1% Triton X-100, 1.2 mM EDTA, 16.7 mM Tris-HCl, pH 8.0, and 167 mM NaCl). The DNA fragments' supernatant was divided into three aliquots. One was the input sample and this was stored in -80°C temporarily. For the other two aliquots, one was incubated with the corresponding antibody as an immunoprecipitation (IP) sample, and the other was incubated with anti-IgG1 (Invitrogen-Thermo Fisher Scientific MA1-10406; Waltham, MA, USA) antibody (mock sample antibody) as a mock sample. Before incubating with antibodies,

protein A agarose beads (Santa Cruz Biotechnology sc-2001; Dallas, TX, USA) were added into IP and mock samples to remove the background that can bind to the agarose beads. The monoclonal anti-GFP (ab290, 1 : 500 dilution; Abcam, Cambridge, UK), anti-H2B ub1 (Cell Signalling Technology 5546, 1 : 500 dilution; Danvers, MA, USA), H3K4 me2 (ab7766, 1 : 500 dilution; Abcam) or H3K4 me3 (ab8580, 1 : 500 dilution; Abcam) was added into IP samples as IP sample antibody in corresponding assays. Then protein A agarose beads were added for

Fig. 1 FgAreA regulates putrescine-promoted the mycotoxin deoxynivalenol (DON) biosynthesis during *Fusarium graminearum* infection.

(a) Concentrations of putrescine and spermidine produced by wheat increased during *F. graminearum* infection. (b) The transcription of putrescine and spermidine biosynthetic genes in wheat was induced during *F. graminearum* infection. Values are the relative expression in inoculated wheat heads compared with uninfected wheat heads at the corresponding time point. dpi, days post-inoculation. (c) Putrescine promoted *in vitro* DON production in *F. graminearum*. (d) Putrescine promoted the transcription of DON biosynthetic genes (*FgTRIs*) in *F. graminearum*. In (c, d), after 24 h culture in yeast extract peptone dextrose (YEPD), strains were transferred to trichothecene biosynthesis-inducing (TBI) medium using putrescine, spermidine or glutamine as the nitrogen source for 7 d (DON determination) or 48 h (*FgTRIs* expression detection). The expression level of each *FgTRI* in the wild-type (PH-1) in TBI with glutamine was set to 1 and the *FgACTIN* gene was used as the internal control for normalization. (e) Putrescine biosynthesis inhibitors decreased DON production in *F. graminearum* during infection on wheat coleoptiles. The amount of DON was determined after 7 dpi, with or without the treatment with putrescine biosynthesis inhibitors 2 mM DL- α -difluoromethylarginine (DFMA) and 2 mM DL- α -difluoromethylornithine (DFMO). (f, g) Putrescine biosynthesis inhibitors reduced *F. graminearum* virulence. Representative images (f) and lesion sizes (g) of wheat coleoptiles treated with or without 2 mM DFMA + 2 mM DFMO after 1, 2, 4 dpi. Arrows indicate the corresponding coleoptiles lesion sites. (h) Putrescine-induced DON production was dependent on the transcription factor FgAreA *in vitro*. (i) Putrescine-induced *FgTRIs* expression relied on FgAreA. In (g, h), DON production and *FgTRIs* expression were determined as indicated in (c, d). (j) Deletion of FgAreA led to dramatically reduced DON production during infection on wheat coleoptiles. The amount of DON produced by PH-1, Δ FgAreA and Δ FgAreA-C on wheat coleoptiles was determined after 7 dpi. (k, l) Deletion of FgAreA caused severe deficiency in virulence. Representative images (k) and lesion sizes (l) of wheat coleoptiles after 4 dpi. Arrows indicate the corresponding coleoptiles lesion sites. Mean and SD were estimated with data from three independent biological replicates (marked with blue dots, $n = 3$). Asterisks indicate statistically significant differences using two-way ANOVA analysis followed by Sidak's multiple comparisons test ($P = 0.05$). Different letters indicate significant differences based on ANOVA analysis followed by Turkey's multiple comparisons test ($P = 0.05$).

a second time for immunoprecipitation in IP and mock samples. The beads were subsequently washed in a low-salt-wash buffer, a high-salt-wash buffer, a LiCl wash buffer and TE buffer. The immunoprecipitated complexes were then eluted from beads with freshly prepared elution buffer (1% sodium dodecyl sulfate (SDS), 0.1 M NaHCO₃). Then 5 M NaCl was added into input, ChIP and mock samples and incubated at 65°C for at least 4 h to overnight to reverse cross-linking. The resulting complexes were treated with 2 μ l RNase/sample at 37°C for 2 h, reversed cross-linking and digested with proteinase K at 45°C for 2 h. For each sample, an equal volume of phenol/chloroform/isoamyl alcohol was added to precipitate DNA at –20°C for 3 h or overnight. Input, IP and mock DNA samples were quantified by quantitative PCR assays with primers listed in Table S1. Relative enrichment levels were determined using the fold enrichment method. The ChIP signals are divided by the mock signals, representing the ChIP signal as the fold increase in signal relative to the background signal. The experiment was repeated three times.

The micrococcal nuclease-qPCR assays

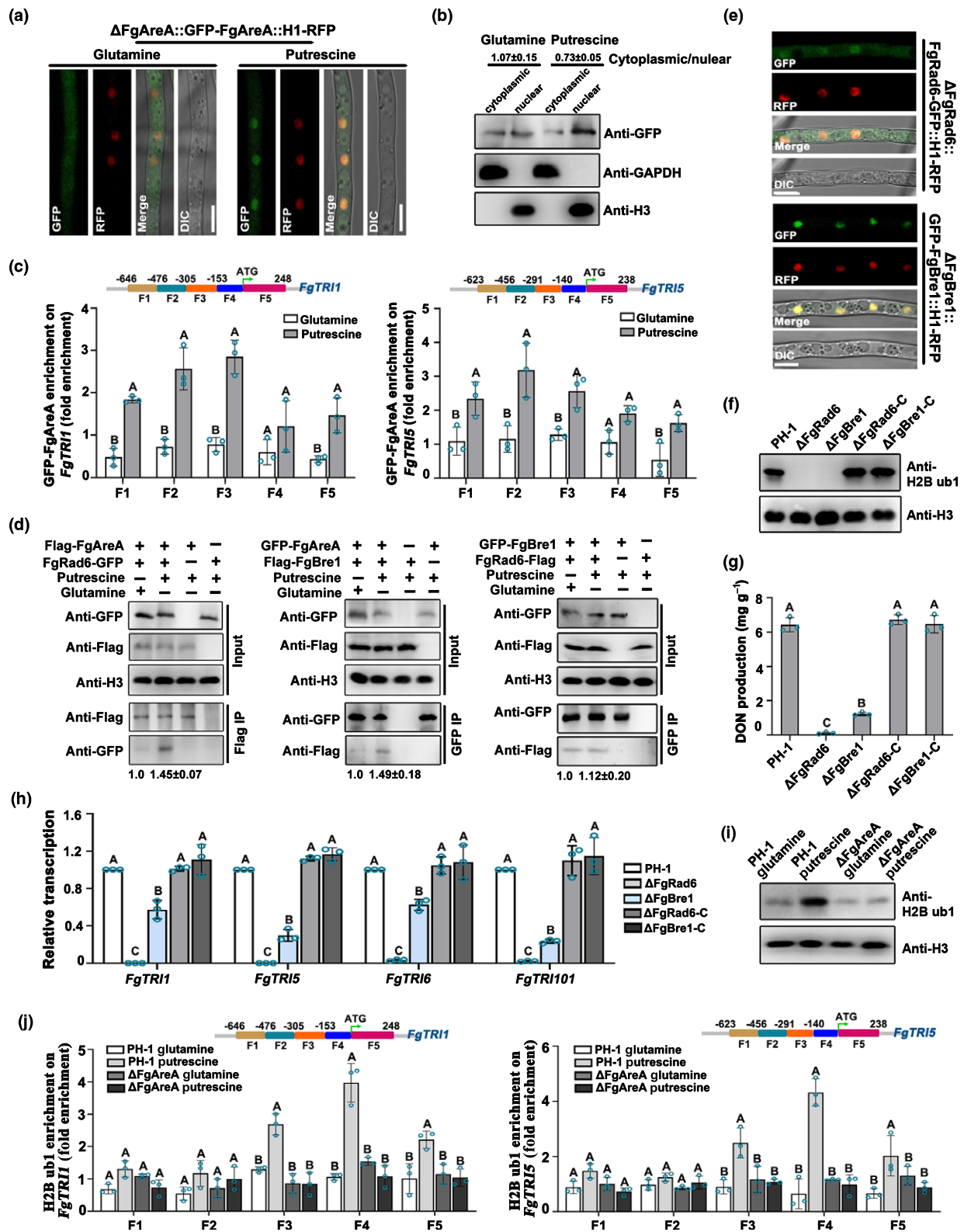
A micrococcal nuclease (MNase) assay was conducted using a previously reported protocol (Kaster & Laubinger, 2016). Briefly, to isolate fungal nuclei, fresh mycelia of each strain were frozen in liquid nitrogen, and ground to a fine powder using a mortar and pestle. The resulting powdered mycelia (0.6 g) were mixed with 1 ml of lysis buffer (250 mM sucrose, 25% (v/v) glycerol, 2 mM MgCl₂, 20 mM KCl, 20 mM Tris–HCl (pH 7.5), 5 mM dithiothreitol) and incubated on ice for 5 min with constant stirring. The homogenates were then filtered through cheesecloth and subsequently centrifuged at 1500 g for 15 min at 4°C. The pellets were resuspended in 1 ml nuclei extraction buffer NEB1 (20 mM Tris–HCl (pH 7.5), 0.2% (w/v) TritonX-100, 25% (v/v) glycerol, 2.5 mM MgCl₂) and centrifuged at 15 000 g for 10 min at 4°C. This step was repeated five times. The resulting pellets were resuspended in 1 ml NEB2 buffer (20 mM Tris–HCl (pH 7.5), 0.5% (w/v) TritonX-100, 250 mM sucrose,

10 mM MgCl₂, 5 mM β -mercaptoethanol), layered onto 1 ml of NEB3 buffer (20 mM Tris–HCl (pH 7.5), 0.5% (w/v) TritonX-100, 1.7 M sucrose, 10 mM MgCl₂, 5 mM β -mercaptoethanol), and centrifuged at 16 000 g for 45 min at 4°C. The final nuclei pellet was suspended in MNase reaction buffer. To conduct MNase digestion, an equal portion of nuclei isolation (160 μ l) of each sample was mixed with 320 μ l MNase reaction buffer and treated with 4 μ l MNase enzyme (Takara, Beijing, China). The same amount of nuclei isolation without MNase treatment was used as an undigested control. Samples were incubated at 37°C for 8 min, and reaction was terminated by adding 50 μ l of stop buffer (50 μ l 10% SDS, and 40 μ g proteinase K) at 60°C for 1 h. Each resulting sample was then treated with 1 U RNase (10 μ g μ l^{–1}) at 37°C for 1 h and stored at 4°C overnight. DNA from each sample was extracted using the phenol-chloroform-isoamyl alcohol method and resuspended in 50 μ l water. The resulting DNA samples were used for quantitative PCR with multiple pairs of primers spanning the tested region (Table S1). The resulting amplicons, having an average size of 100 with 20 bp overlap, were used for analyzing nucleosome occupancy as described previously (Kaster & Laubinger, 2016).

Results

Deoxynivalenol production induced by putrescine is dependent on FgAreA during *F. graminearum* infection

Polyamines produced by the host have been found to be involved in DON production during *F. graminearum* infection (Gardiner *et al.*, 2009, 2010; Kazan *et al.*, 2012; Bonnighausen *et al.*, 2019). To determine which polyamine(s) function in DON biosynthesis, we first inoculated wheat heads with *F. graminearum* conidia and measured the concentrations of three main polyamines, putrescine, spermidine and spermine, from infected wheat heads. As shown in Fig. 1(a), the amount of putrescine in the infected spikes increased rapidly and remained elevated from 1 to 7 dpi. Whereas the content of spermidine was slightly increased



at 1, 6 and 7 dpi, the spermine content did not change significantly (Fig. 1a). Next, we detected the transcription levels of five key polyamine biosynthetic enzymes at 1–7 dpi. Ornithine decarboxylase (ODC) and arginine decarboxylase 2 (ADC2) are

responsible for putrescine biosynthesis, S-adenosylmethionine (SAM) is important for the biosynthesis of both spermidine and spermine, spermidine synthase 1 (SPDS1) and spermidine synthase 2 (SPDS2) are responsible for spermidine biosynthesis

Fig. 2 FgAreA induces *FgTRI*s transcription via increasing H2B ub1 enrichment upon putrescine treatment. (a) Green fluorescent protein (GFP)-FgAreA accumulated in the nucleus after treatment with putrescine. The strain was grown in yeast extract peptone dextrose (YEPD) for 24 h, then transferred to trichothecene biosynthesis-inducing (TBI) medium with putrescine or glutamine for 6 h. Red fluorescent protein (RFP)-tagged histone 1 (H1) acted as the nucleus marker. Bars, 10 μ m. (b) Western blot assays confirmed nuclear accumulation of GFP-FgAreA upon putrescine treatment. For protein extraction, the strain Δ FgAreA::GFP-FgAreA was grown in TBI with putrescine or glutamine for 6 h after 24 h culture in YEPD. Nuclear and cytoplasmic fractions were detected with the anti-GFP antibody. The intensity of GFP-FgAreA in the nucleus is relative to the amount of H3, while the intensity of GFP-FgAreA in the cytoplasm is relative to the amount of GAPDH. The intensities of the Western blot bands were quantified with IMAGEJ. (c) Chromatin immunoprecipitation-quantitative PCR (ChIP-qPCR) assays showed that putrescine induced GFP-FgAreA binding to the promoters of *FgTRI* genes. (d) Coimmunoprecipitation (Co-IP) assays showed that FgAreA interacted with both FgRad6 and FgBre1 and the interactions were enhanced by putrescine treatment. FgRad6 also interacted with FgBre1 in the Co-IP assay. The strains were cultured in YEPD for 24 h, and then transferred to TBI with putrescine or glutamine for 48 h. Total proteins (input) extracted from the strain containing a pair of constructs or a single construct were subjected to sodium dodecyl sulfate-polyacrylamide gel electrophoresis and immune blots were incubated with the monoclonal anti-GFP and anti-Flag antibodies for detection of GFP/Flag-FgAreA, FgRad6-GFP/Flag, and GFP/Flag-FgBre1, respectively, as indicated. Then, each protein sample was pulled down using anti-GFP or anti-Flag agarose and further detected with these antibodies. The protein samples were also detected with anti-H3 antibody as a reference. The intensities of the Western blotting bands were quantified with IMAGEJ. Values on the bars are the intensity of detected protein band relative to that of the H3 band. (e) FgRad6-GFP and FgBre1-GFP both colocalized with RFP-tagged nucleus marker H1 in TBI with putrescine. Bars, 10 μ m. (f) Western blot assays showed that FgRad6 and FgBre1 regulated H2B ub1 level. H2B ub1 level was detected with the anti-H2B ub1 antibody. H3 level detected with anti-H3 antibody was conducted as the protein loading reference. (g) Deletion of FgRad6 or FgBre1 led to reduced deoxynivalenol (DON) production. (h) Deletion of FgRad6 or FgBre1 caused decreased *FgTRI*s expression. (i) Western blot assays showed that putrescine treatment increased global H2B ub1 level, and the increased H2B ub1 level was dependent on FgAreA. For protein extraction, PH-1 and Δ FgAreA were grown in YEPD for 24 h, and then transferred to TBI with putrescine or glutamine for 48 h. (j) ChIP-qPCR assays revealed that putrescine treatment increased H2B ub1 enrichment on *FgTRI* promoters, and the increased H2B ub1 enrichment relied on FgAreA. In (c, j), strains were grown in TBI with putrescine or glutamine for 48 h after 24 h culture in YEPD. ChIP and mock DNA samples were quantified by quantitative PCR assays with primers amplifying different regions indicated on the diagram of each *FgTRI* promoter. Relative enrichment levels were determined using the fold-enrichment method. The ChIP signals are divided by the mock signals, representing the ChIP signal as the fold increase in signal relative to the background signal. Mean and SD were estimated with data from three independent biological replicates (marked with blue dots, $n = 3$). Different letters indicate significant differences based on ANOVA analysis followed by Turkey's multiple comparisons test ($P = 0.05$).

(Cynthia *et al.*, 2004). Quantitative reverse transcription polymerase chain reaction (qRT-PCR) assays showed that the transcription levels of *TaODC* and *TaADC2* were significantly increased after inoculation, whereas the transcription levels of *TaSPDS1* and *TaSPDS2* were more variable and only slightly increased during infection (Fig. 1b). Moreover, no significant difference was observed in *TaSAM* transcription level in infected wheat heads relative to healthy wheat heads (Fig. 1b). These results suggest that putrescine and spermidine might regulate DON biosynthesis during infection.

Further, we examined the effect of putrescine and spermidine on DON production using trichothecene biosynthesis-inducing (TBI) medium (Gardiner *et al.*, 2009) with each of them as the sole nitrogen source. Meanwhile, the primary nitrogen source, glutamine, was used as a control, as it does not induce DON production (Gardiner *et al.*, 2009). As shown in Fig. 1(c), putrescine significantly increased DON production, while spermidine did not induce DON production. Next, qRT-PCR data revealed that the transcriptional expressions of *FgTRI1*, *FgTRI5*, *FgTRI6* and *FgTRI101* were significantly increased using putrescine as sole nitrogen source (Fig. 1d). These results indicated that putrescine contributed to DON production *in vitro*.

To further verify that putrescine plays a key role in triggering DON biosynthesis in *F. graminearum* during infection, we determined the DON content in infected wheat coleoptiles treated with putrescine biosynthesis inhibitors DL- α -difluoromethylarginine (DFMA) and DL- α -difluoromethylornithine (DFMO) (Ma & Li, 2010; Yamamoto *et al.*, 2017). As shown in Fig. 1(e), DON production was significantly reduced in DFMA and DFMO treated coleoptiles compared with untreated coleoptiles. Accordingly, the stems of DFMA- and DFMO-treated coleoptiles displayed shorter

brown necrotic lesions than those of control coleoptiles (Fig. 1f,g), further supporting the idea that DON is a key virulence factor during infection. In addition, given that endogenous putrescine was reported to be able to accelerate DON production in *F. graminearum* (Crespo-Sempere *et al.*, 2015), we also tested the transcriptional changes of fungal putrescine synthetase *FgODC* (*FGSG_05903*) during infection. We found that the transcription level of *FgODC* decreased (Fig. S1), suggesting that for *F. graminearum*, endogenous putrescine synthesis may not play an important role in enhancing DON production during infection. These results indicate that accumulated putrescine produced by the host stimulates DON production in *F. graminearum* during infection.

FgAreA as a regulator of secondary nitrogen source utilization has been found to be involved in DON production (Min *et al.*, 2012; Yu *et al.*, 2014; Hou *et al.*, 2015). Thus, we were interested in whether DON production induced by putrescine was associated with FgAreA during infection. As shown in Fig. 1(h), DON production was reduced dramatically in Δ FgAreA compared with the wild-type and complemented strain Δ FgAreA-C in TBI with putrescine. Consistent with this, qRT-PCR assays revealed that the expression levels of *FgTRI1*, *FgTRI5*, *FgTRI6* and *FgTRI101* in Δ FgAreA were also significantly decreased (Fig. 1i). Moreover, *in vivo* coleoptile inoculation assays showed that DON was not produced in Δ FgAreA, and the lesion lengths were dramatically shortened on coleoptile stems inoculated with Δ FgAreA compared with the wild-type and Δ FgAreA-C (Fig. 1j–l). Further, we analyzed DON production in TBI with glutamine supplemented with a DON-inducing carbon source sucrose, or a noninducing carbon source glucose, to exclude the possibility that FgAreA is also responsive to other factors. We

found that deletion of *FgAREA* did not affect sucrose-mediated induction in DON biosynthesis (Fig. S2). These results strongly indicated that FgAreA is necessary for putrescine-induced DON biosynthesis.

FgAreA modulates *FgTRIs* transcription by upregulating H2B ub1 enrichment upon putrescine treatment

To explore how FgAreA modulates DON biosynthesis upon putrescine treatment, we first checked the transcription, protein quantity and localization of FgAreA in TBI supplemented with putrescine compared with those in TBI supplemented with glutamine. Confocal microscopic examination showed that FgAreA entered into the nucleus upon putrescine treatment (Fig. 2a,b), although the total protein quantity and transcription levels were not altered (Fig. S3). Further, chromatin immunoprecipitation and quantitative PCR (ChIP-qPCR) analyses revealed that the enrichment of FgAreA on *FgTRIs* was elevated in TBI with putrescine compared with that in TBI with glutamine (Fig. 2c). Overall, these results indicate that the nuclear localization and enrichment at target genes contribute to the transcriptional activity of FgAreA.

In eukaryotic organisms, the process of transcription takes place on chromatin in cooperation with multiple transcription factors that impact Pol II activity, mediate responses to additional regulatory proteins or modify the chromatin template (Woodworth & Holloway, 2016; Sood *et al.*, 2017). To further explore the function of FgAreA in regulating *FgTRIs* transcription under putrescine treatment, we identified the FgAreA-interacting proteins in TBI with putrescine using an affinity capture assay. Briefly, FgAreA with the N-terminus fused with GFP was transferred into Δ FgAreA. The proteins purified with GFP-trap agarose beads were further analyzed by MS. The FgAreA-interacting proteins were identified and annotated by searching the MS data against *F. graminearum* PH-1 (NCBI_assembly ASM24013v3). False discovery rate (FDR) was used to determine relative protein confidence, and peptide-to-spectrum matches (PSMs) were quantified to determine relative protein abundance (Kruger *et al.*, 2019). A total of 576 candidate-interacting proteins with $\leq 1\%$ FDR and PSM > 5 were listed in the Table S2. We scanned for transcription-related proteins such as histone modifiers, transcription factors or elongation factors among the 576 candidates, and then focused on the putative H2B ub1 conjugating enzyme FgRad6 (FGSG_12683) and ligase enzyme FgBre1 (FGSG_06769). The interactions of FgAreA with FgRad6 and FgBre1 were further confirmed by coimmunoprecipitation (Co-IP) assays (Fig. 2d). Moreover, the interactions of FgAreA with FgRad6 and FgBre1 were stronger in TBI with putrescine than in TBI with glutamine (Fig. 2d), and FgRad6 also interacts with FgBre1 in the Co-IP assay, suggesting the association between H2B ub1 and FgAreA plays a vital role in the presence of putrescine. Accordingly, FgRad6-GFP, GFP-FgBre1 and GFP-FgAreA showed colocalization with the red fluorescent protein (RFP) signals of nuclear marker histone 1 (H1) in TBI with putrescine (Fig. 2a,e), further indicating their function in transcriptional regulation. To confirm that FgRad6 and

FgBre1 are responsible for H2B ub1, we generated the deletion mutants for *FgRAD6* and *FgBRE1* (Fig. S4), and found that H2B ub1 level was not detected in the mutants Δ FgRad6 and Δ FgBre1 (Fig. 2f), indicating that FgRad6 and FgBre1 are responsible for H2B ub1 biogenesis in *F. graminearum*. These data suggest that H2B ub1 might be involved in FgAreA-regulated transcription of *FgTRIs*.

To explore whether H2B ub1 participates in FgAreA-regulated DON biosynthesis upon putrescine treatment, we first determined the concentration of DON and transcriptional expression of *FgTRIs* in Δ FgRad6 and Δ FgBre1 mutants. As shown in Fig. 2, DON content in Δ FgRad6 and Δ FgBre1 was significantly reduced in TBI by putrescine treatment, as compared with the wild-type and complemented strains (Δ FgRad6-C and Δ FgBre1-C), respectively. Also, the transcriptional expressions of *FgTRI1*, *FgTRI5*, *FgTRI6* and *FgTRI101* genes were dramatically decreased in Δ FgRad6 and Δ FgBre1 (Fig. 2h). Furthermore, we detected the effects of putrescine on H2B ub1 levels in TBI, using glutamine as a control. Western blot assays revealed that the application of putrescine facilitated H2B ub1, as compared with glutamine; meanwhile, FgAreA is required for the induction of the increased H2B ub1 in TBI by putrescine treatment (Fig. 2i). ChIP-qPCR analysis showed that the enrichments of H2B ub1 on *FgTRI1* and *FgTRI5* under putrescine induction were significantly higher than those in TBI with glutamine (Fig. 2j). Obviously, the enhancement of H2B ub1 on *FgTRI1* and *FgTRI5* by putrescine was compromised in the *FgAREA* loss-of-function mutant (Fig. 2j), which is consistent with the reduced transcriptional expressions of *FgTRI1* and *FgTRI5* in Δ FgAreA (Fig. 1h). These results indicate that FgAreA enters into the nucleus in responding to putrescine, and then facilitates H2B ub1 enrichment on *FgTRIs*, consequently resulting in *FgTRIs* transcriptional activation.

The bZIP domain of FgBre1 is required for H2B ub1 biogenesis

Previous studies have found that Bre1 is important for positioning Rad6 to the monoubiquitination site at H2B Lys123 in yeast (Wood *et al.*, 2003; Gallego *et al.*, 2016), but the mechanism by which Bre1 recognizes the target chromosome is poorly understood. Analyzing the domains of FgRad6 and FgBre1, FgRad6 shares high homology with other eukaryotic organisms (Fig. S5); however, it was surprising to find that FgBre1 contains a basic region leucine zipper (bZIP) domain (Fig. 3a). Given that the bZIP is a typical sequence-specific DNA-binding domain (Beresova *et al.*, 2009), we therefore speculated that FgBre1 may function in selecting the target chromatin of H2B ub1 by way of its specific DNA-binding ability. Phenotypic characterization of a strain lacking the bZIP domain (Δ FgBre1-C^{AbZIP}) showed that, similar to Δ FgBre1, Δ FgBre1-C^{AbZIP} displayed the defects in H2B ub1 modification, mycelia growth, DON biosynthesis and *FgTRIs* transcription (Fig. 3b–e). Further, ChIP-qPCR assays revealed reduced H2B ub1 enrichment on *FgTRI1* and *FgTRI5* in Δ FgBre1-C^{AbZIP} compared with Δ FgBre1-C (Fig. 3f). Consistent with that observation, binding of FgBre1 on *FgTRI1* and

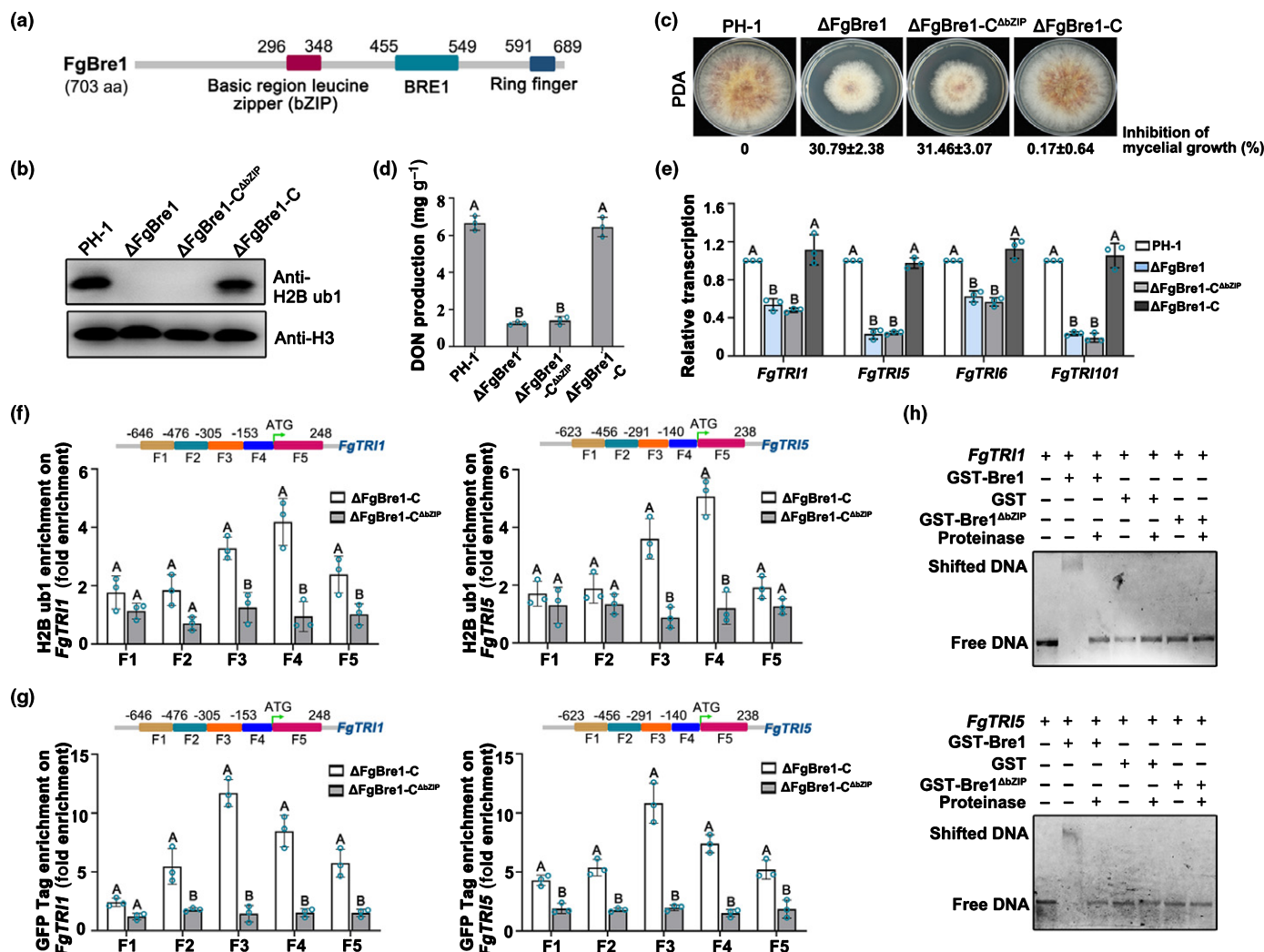


Fig. 3 The basic region leucine zipper (bZIP) domain is required for FgBre1 binding to target chromatin. (a) FgBre1 contains a specific DNA-binding domain, bZIP, as analyzed using the SMART protein database (<http://smart.embl-heidelberg.de>). (b) Western blot assays showed that the lack of the bZIP domain disrupted the generation of H2B ub1. (c) Lack of the bZIP domain caused a defect in mycelial growth. Colony morphology was observed after growth on potato dextrose agar (PDA) for 3 d. (d) Deletion of the bZIP domain led to decreased deoxynivalenol (DON) production in trichothecene biosynthesis-inducing (TBI) medium with putrescine. (e) Deletion of the bZIP domain resulted in reduced transcription of *FgTRI* genes under putrescine treatment. (f) Chromatin immunoprecipitation-quantitative PCR (ChIP-qPCR) assays showed that the bZIP domain was indispensable for the enrichment of H2B ub1 at the promoters of *FgTRI* genes. (g) ChIP-qPCR assays showed that the bZIP domain was required for the enrichment of the green fluorescent protein (GFP)-tagged FgBre1 at the promoters of *FgTRI* genes. In (d–g) strains were grown in TBI with putrescine for 48 h after 24 h culture in yeast extract peptone dextrose (YEPD). Mean and SD were estimated with data from three independent biological replicates (marked with blue dots, $n = 3$). Different letters indicate significant differences based on ANOVA analysis followed by Turkey's multiple comparisons test ($P = 0.05$). In (f, g), relative enrichment levels were determined using the fold-enrichment method. (h) Electrophoretic mobility shift assay (EMSA) verified the binding of FgBre1 with *FgTRIs* promoters relied on bZIP domain.

FgTRI5 was not observed in the bZIP domain truncated strain (Fig. 3g). Moreover, electrophoretic mobility shift assays (EMSAs) confirmed that FgBre1 can bind *FgTRI1* and *FgTRI5*, but FgBre1 lacking the bZIP domain cannot (Fig. 3h). Taken together, the bZIP domain of FgBre1 mediates the binding of target genes, which is indispensable for H2B ub1 positioning in *F. graminearum*.

In eukaryotic organisms, H2B ub1 mediated by Rad6 and Bre1 is highly conserved (Fuchs & Oren, 2014). However, we found that the bZIP domain exists exclusively in *Fusarium* species, but not in the Bre1 homologs of human, *Drosophila*, yeasts and other filamentous fungi (Fig. 4a). Thus we were

interested in exploring functional differences of Bre1 homologs with or without the bZIP domain. The full-length cDNAs of *F. verticillioides* FvBre1, *Botrytis cinerea* BcBre1 and *Drosophila melanogaster* DmBre1 tagged with GFP were transformed into the Δ FgBre1 to generate heterologous Bre1 complementation strains Δ FgBre1-C^{Fv}, Δ FgBre1-C^{Bc} and Δ FgBre1-C^{Dm}, respectively. Western blot analysis showed that the heterologous Bre1 proteins were expressed in Δ FgBre1-C^{Fv}, Δ FgBre1-C^{Bc} and Δ FgBre1-C^{Dm} (Fig. 4b). However, only Δ FgBre1-C and Δ FgBre1-C^{Fv} strains restored H2B ub1 modification of Δ FgBre1; the H2B ub1 level was undetectable in Δ FgBre1-C^{Bc} and Δ FgBre1-C^{Dm} (Fig. 4b). Further phenotype determination

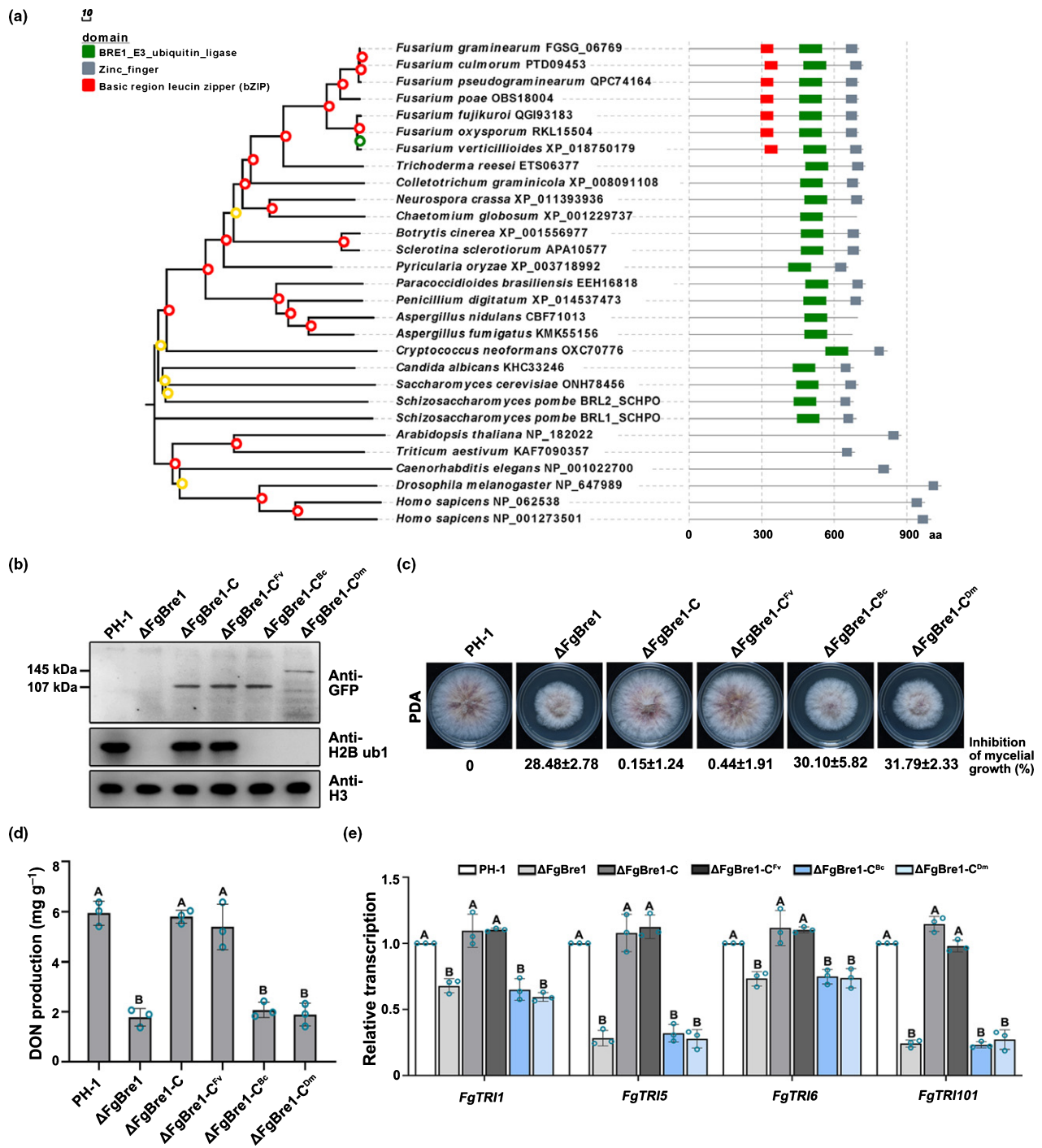


Fig. 4 The basic region leucine zipper (bZIP) domain of Bre1 exists exclusively in *Fusarium* species. (a) The homology among Bre1 orthologs from 27 eukaryotic species was analyzed using the protein BLAST tool on the NCBI platform (<https://blast.ncbi.nlm.nih.gov/Blast.cgi>). The phylogenetic tree was constructed based on the Bre1 amino acid sequences from 27 species with MEGA 5.0 using the neighbor-joining method. The bootstrap values from 1000 replications are indicated using color-coded circles at the branches. Green circle, 0–50; yellow circle, 50–80; red circle, 81–100. Conserved domains in Bre1 orthologs (right panel) were predicted with the SMART program (<http://smart.embl-heidelberg.de>). (b) Western blot assays showed that heterologous Bre1 proteins without the bZIP domain could not recover the H2B ub1 deficiency of $\Delta FgBre1$, whereas Bre1 proteins from *Fusarium* with the bZIP domain restored the H2B ub1 level of $\Delta FgBre1$. The successful expression of Bre1 orthologs in corresponding complementary strains was detected by the anti-green fluorescent protein (GFP) antibody. H3 level detected with an anti-H3 antibody was used as the protein loading reference. (c–e) Heterologous Bre1 proteins without the bZIP domain could not restore defects in mycelia growth (c), deoxynivalenol (DON) production (d) and *FgTRI*s transcription (e), whereas Bre1 proteins from *Fusarium* with the bZIP domain restored these defects of $\Delta FgBre1$. Colony morphology was observed after culture on potato dextrose agar (PDA) for 3 d. For DON production and *FgTRI*s transcription, strains were grown in trichothecene biosynthesis-inducing (TBI) medium with putrescine for 48 h after 24 h culture in yeast extract peptone dextrose (YEPD). Mean and SD were estimated with data from three independent biological replicates (marked with blue dots, $n = 3$). Different letters indicate significant differences based on ANOVA analysis followed by Turkey's multiple comparisons test ($P = 0.05$).

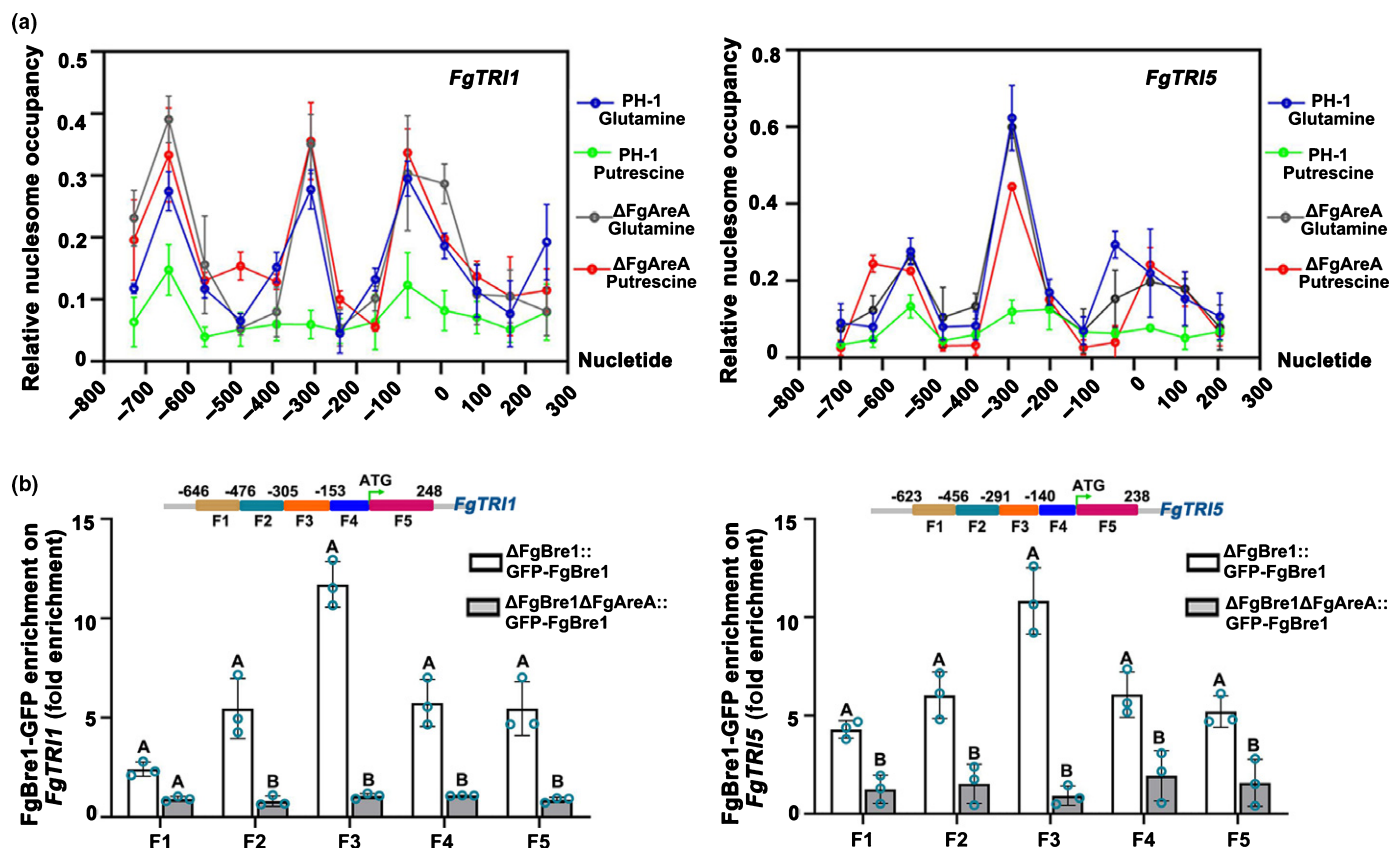


Fig. 5 FgAreA enhances FgBre1's binding to the promoters of *FgTRIs* via mediating chromatin rearrangement. (a) Micrococcal nuclease-quantitative PCR (MNase-qPCR) assays showed that FgAreA mediates nucleosomal positioning rearrangement in deoxynivalenol (DON) biosynthetic gene (*FgTRIs*) promoters. *FgTRI1* and *FgTRI5* upstream were packaged in a positioned array of nucleosomes in trichothecene biosynthesis-inducing (TBI) medium with glutamine (blue), while in TBI with putrescine (green) the positioned nucleosome array was lost, allowing for exposure of a nucleosome-free region. However, the positioned nucleosome array persisted in Δ FgAreA in TBI with glutamine (gray) or putrescine (red). (b) Chromatin immunoprecipitation-quantitative PCR (ChIP-qPCR) assays showed that deletion of FgAreA decreased the enrichment of FgBre1-GFP at the promoters of *FgTRI* genes under putrescine treatment. Strains were grown in yeast extract peptone dextrose (YPD) for 24 h, then transferred to TBI with putrescine for 48 h. Relative enrichment levels were determined using the fold-enrichment method. Mean and SD were estimated with data from three independent biological replicates (marked with blue dots, $n = 3$). Different letters indicate significant differences based on ANOVA analysis followed by Turkey's multiple comparisons test ($P = 0.05$).

showed that BcBre1 and DmBre1 were unable to restore the deficiency in mycelia growth, DON biosynthesis or *FgTRIs* transcription, whereas FvBre1 recovered all the defects of Δ FgBre1 (Fig. 4c–e). These results indicate that the bZIP domain of Bre1 specifically functions in targeting chromosome recognition in *Fusarium* species.

FgAreA accelerates FgBre1's binding to the *FgTRIs*

Although H2B ub1 biogenesis is dependent on the bZIP domain of FgBre1, the molecular mechanism by which FgAreA regulates H2B ub1 occurrence on *FgTRIs* under putrescine induction is still obscure. We therefore analyzed the changes in nucleosomal positioning under *FgTRIs* activation and suppressive conditions in the wild-type and Δ FgAreA. The micrococcal nuclease (MNase)-qPCR assays showed that DNA of *FgTRI1* and *FgTRI5* upstream was packaged in a positioned array of nucleosomes under *FgTRIs* suppressive conditions (TBI with glutamine), while the positioned nucleosome array was lost with exposure of nucleosome-free region during *FgTRIs* activation conditions

(TBI with putrescine) (Fig. 5a). However, the positioned nucleosome array persisted under putrescine treatment in Δ FgAreA (Fig. 5a), indicating that FgAreA modulates chromatin remodeling in the promoters of *FgTRIs* upon putrescine treatment. Further, ChIP-qPCR assays revealed that the highest FgBre1 enrichment regions were distributed in the exposed, nucleosome-free region rearranged by FgAreA (Figs 3g, 5a). Accordingly, ChIP-qPCR assays revealed that the binding of FgBre1 to *FgTRIs* relies on the presence of FgAreA (Fig. 5b). Therefore, we deduced that FgAreA regulates H2B ub1 enrichment on *FgTRIs* by facilitating binding of FgBre1 to *FgTRIs* in the presence of putrescine.

H2B ub1 and H3K4 me2/3 coregulate DON biosynthesis upon putrescine treatment

In eukaryotes, H2B ub1 has been reported to be the prerequisite of H3K4 and histone 3 lysine 79 (H3K79) trimethylations (Kim *et al.*, 2009; Chandrasekharan *et al.*, 2010; Shilatifard, 2012). The H3K4 methyltransferase FgSet1 has been found to regulate the transcription of *FgTRIs* in *F. graminearum* (Liu *et al.*, 2015).

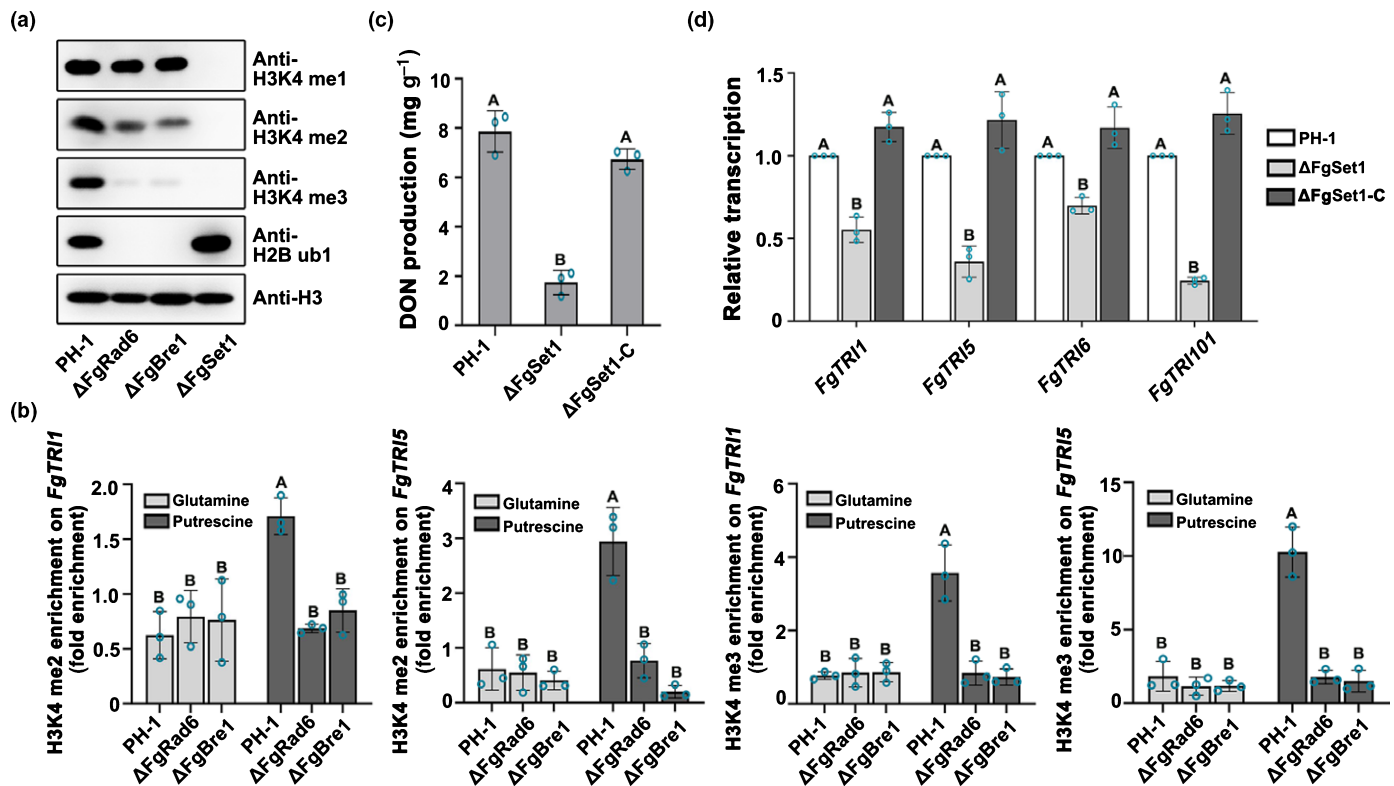


Fig. 6 H2B ub1 and downstream H3K4 me2/3 coregulate deoxynivalenol (DON) biosynthesis under putrescine treatment. (a) Western blot assays showed that the H3K4 me2/3 levels were dramatically reduced in Δ FgRad6 and Δ FgBre1. H3 level detected with anti-H3 antibody was conducted for the protein loading reference. (b) Chromatin immunoprecipitation-quantitative PCR (ChIP-qPCR) assays showed that putrescine treatment increased H3K4 me2 and H3K4 me3 enrichments on the *FgTRI*s 5' regions, and the increased enrichments were dependent on FgRad6 and FgBre1. Relative enrichment levels were determined using the fold-enrichment method. (c) DON production was decreased in Δ FgSet1 in trichothecene biosynthesis-inducing (TBI) medium with putrescine. (d) *FgTRI*s expression was reduced in Δ FgSet1 in TBI with putrescine. In (b–d), the wild-type, mutants Δ FgRad6, Δ FgBre1 and Δ FgSet1, and complemented strain Δ FgSet1-C were grown in TBI with putrescine or glutamine for 48 h after 24 h culture in yeast extract peptone dextrose (YEPD). Mean and SD were estimated with data from three independent biological replicates (marked with blue dots, $n = 3$). Different letters indicate significant differences based on ANOVA analysis followed by Turkey's multiple comparisons test ($P = 0.05$).

Therefore, we were interested in analyzing whether H2B ub1 and H3K4 me1/2/3 synergistically modulate DON biosynthesis under putrescine induction. First, Western blotting assays showed that lack of FgRad6 or FgBre1 dramatically reduced the H3K4 me3 level and, to a lesser extent, decreased the H3K4 me2 level compared with those in the wild-type (Fig. 6a). Whereas the H2B ub1 level in Δ FgSet1 was similar to that in the wild-type (Fig. 6a), it indicates that H3K4 me1/2/3 is not required for H2B ub1 in *F. graminearum*. Further, ChIP-qPCR analyses revealed that H3K4 me2/3 enrichment on *FgTRI1* and *FgTRI5* was increased by putrescine treatment, and was dependent on the presence of FgRad6 and FgBre1, although the global H3K4 me2/3 level was not changed upon putrescine treatment (Figs 6b, S6). As expected, putrescine failed to induce DON production and *FgTRI*s transcription in the mutant Δ FgSet1 (Fig. 6c,d). These results indicate that H2B ub1 collaborated with its downstream H3K4 me2/3 in regulating DON biosynthesis upon putrescine treatment.

FgBre2 links H2B ub1 to H3K4 me2/3

Given that the molecular mechanism of H2B ub1 regulating H3K4 me2/3 is controversial and poorly understood (Zheng

et al., 2018; Hsu *et al.*, 2019; Bae *et al.*, 2020), we were interested in exploring how H2B ub1 modulates the biogenesis of H3K4 me2/3. H3K4 me2/3 is regulated by the methyltransferase complex COMPASS that consists of eight subunits, Set1, Bre2 (Cps60), Swd1 (Cps50), Spp1 (Cps40), Swd2 (Cps35), Swd3 (Cps30), Sdc1 (Cps25) and Shg1 (Cps15), in *S. cerevisiae* (Shilatifard, 2012). Thus, we first identified these components by BLASTP searching for the corresponding orthologs of *S. cerevisiae* COMPASS components in the *F. graminearum* genome database (<http://fungidb.org/fungidb/>) (Table S3). Western blotting assays showed that FgSet1, FgSwd1, FgSwd3, FgSdc1 and FgBre2 were all involved in H3K4 me2/3 generation, DON production and *FgTRI*s transcription (Fig. S7a–c). Next, we detected the interaction between FgRad6 and FgBre1 with the COMPASS components using the yeast two-hybrid (Y2H) approach. As shown in Figs 7(a) and S8(a), FgRad6 and FgBre1 both interact with FgSet1 and FgBre2, but not other COMPASS components. The Co-IP assays further verified the interaction between FgSet1 and FgBre2 with FgRad6 and FgBre1 (Fig. 7b).

To explore the potential roles of these interactions in H2B ub1 regulating H3K4 me2/3, we first detected ubiquitylation levels of FgSet1 and FgBre2, as FgRad6 and FgBre1 serve as ubiquitylation E2 conjugating enzyme and E3 ligase, respectively. As shown

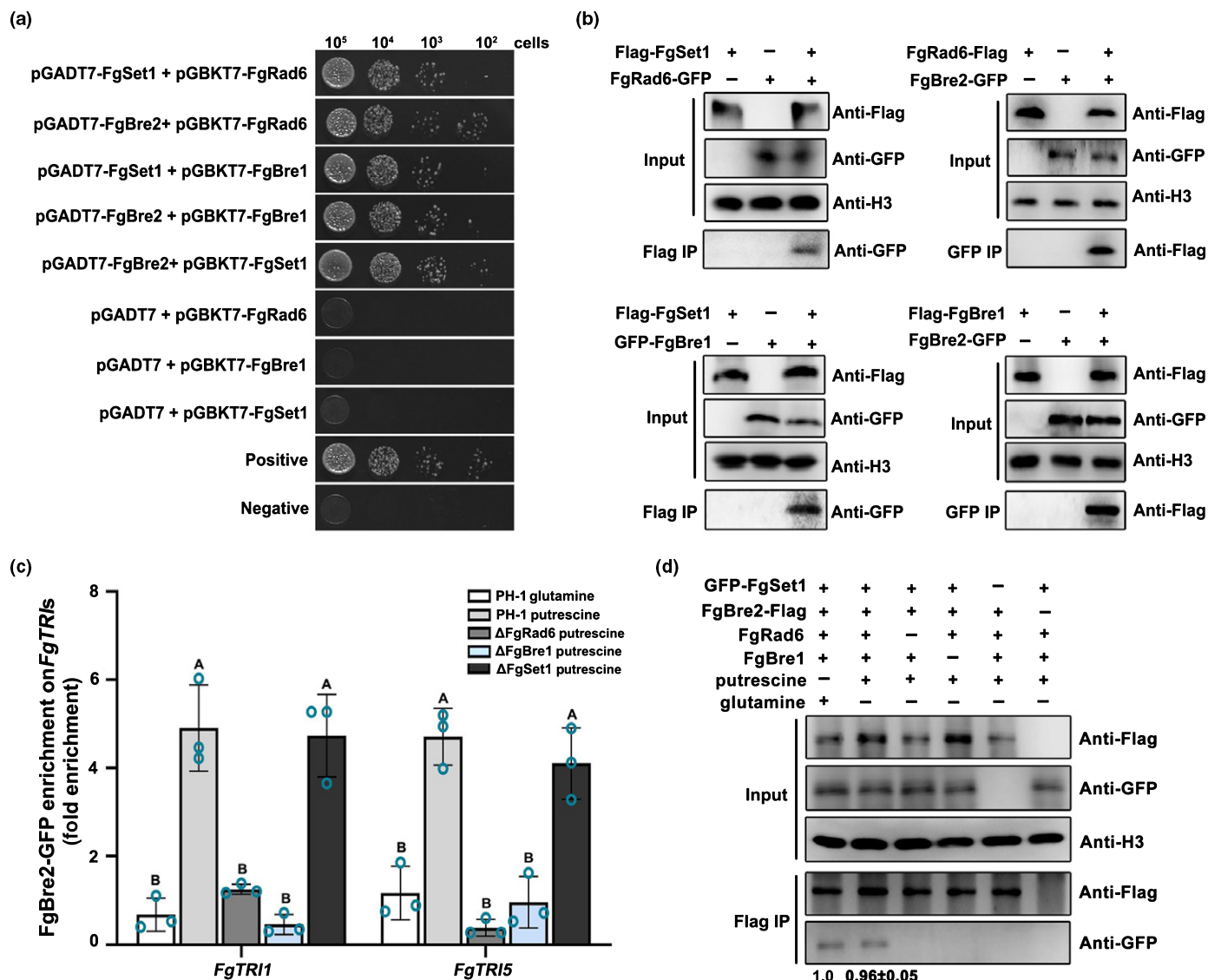


Fig. 7 FgRad6 and FgBre1 regulate H3K4 me2/3 via facilitating the interaction of FgBre2 and FgSet1. (a) Yeast two-hybrid (Y2H) assays showed that both FgRad6 and FgBre1 interact with FgBre2 and FgSet1, and FgBre2 also interacts with FgSet1. (b) Coimmunoprecipitation (Co-IP) assays showed that both FgRad6 and FgBre1 interact with FgBre2 and FgSet1. (c) Chromatin immunoprecipitation-quantitative PCR (ChIP-qPCR) assays showed that the enrichment of FgBre2-GFP on the 5' regions of *FgTRIs* increased upon putrescine treatment. Deletion of FgRad6 and FgBre1 blocked the increase of FgBre2-GFP enrichment on *FgTRIs* upon putrescine treatment. Strains were grown in yeast extract peptone dextrose (YEED) for 24 h, and then transferred to trichothecene biosynthesis-inducing (TBI) medium with putrescine or glutamine for 48 h for ChIP-qPCR assays. Relative enrichment levels were determined using the fold-enrichment method. Mean and SD were estimated with data from three independent biological replicates (marked with blue dots, $n = 3$). Different letters indicate significant differences based on ANOVA analysis followed by Turkey's multiple comparisons test ($P = 0.05$). (d) Lack of FgRad6 or FgBre1 impeded the interaction of FgBre2 and FgSet1. The Co-IP assays also showed that the interaction between FgBre2 and FgSet1 was not enhanced by putrescine treatment. The strain was cultured in YEED for 24 h, and then transferred to TBI with putrescine or glutamine for 48 h. The protein samples were also detected with anti-H3 antibody as a reference. The intensities of the Western blotting bands were quantified with IMAGEJ. Values on the bars are the intensity of detected protein band relative to that of H3 band.

in Fig. S8(b), neither of them could be monoubiquitinated by FgRad6 and FgBre1. Second, we detected protein concentrations of FgSet1 and FgBre2 in Δ FgRad6 and Δ FgBre1 as protein interactions might affect the stability of interacting proteins. However, we found that deletion of FgRad6 and FgBre1 did not affect the protein stability of FgSet1 and FgBre2 (Fig. S8c). Third, the Y2H and Co-IP assays showed that FgSet1 interacts with FgBre2 (Fig. 7a,d). Given that Set1 methyltransferase activity is affected by its interaction with Bre2 in mammals (Cao *et al.*,

2010), we therefore determined whether FgRad6 and FgBre1 modulate H3K4 me2/3 via interference with the interaction between FgSet1 and FgBre2. As shown in Fig. 7(d), lack of FgRad6 or FgBre1 impeded their interaction. Fourth, ChIP-qPCR assays revealed that the enrichment of FgBre2 on *FgTRI1* and *FgTRI5* was induced under TBI with putrescine and was dependent on the presence of FgRad6 and FgBre1. Nevertheless the enrichment of FgSet1 on *FgTRI1* and *FgTRI5* showed no significant difference under TBI with putrescine and glutamine and

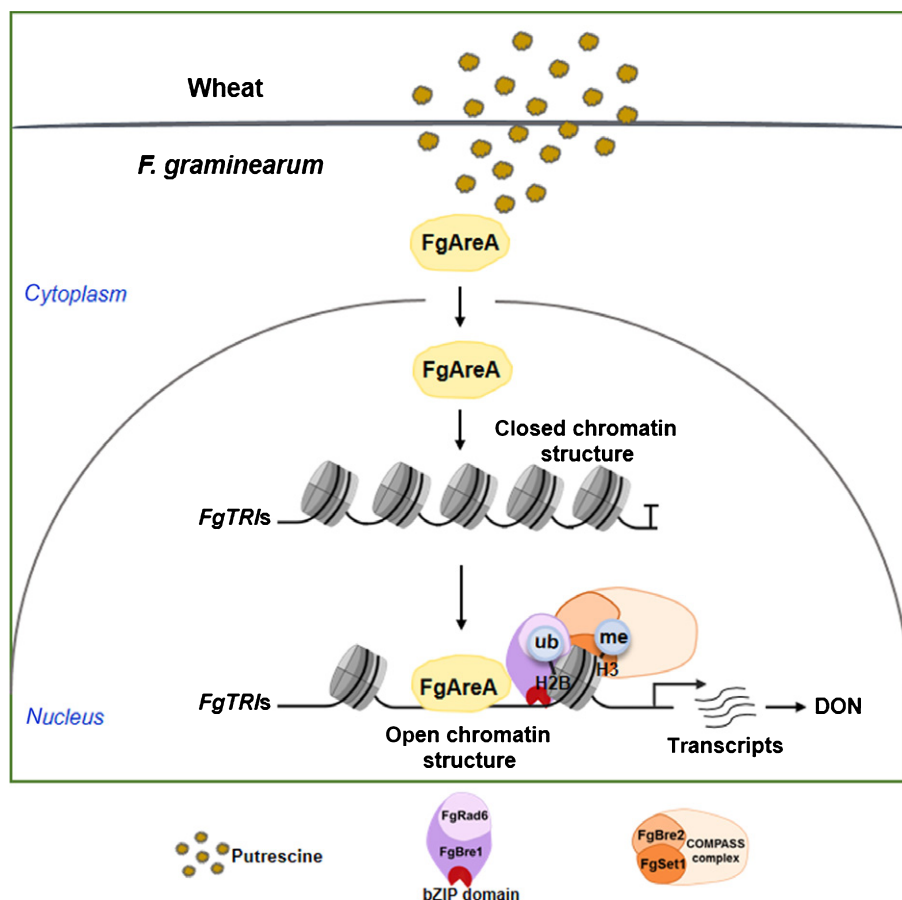


Fig. 8 Proposed model for the molecular mechanism of putrescine-promoted deoxynivalenol (DON) production in *Fusarium graminearum* during infection. Wheat produces substantial putrescine during *F. graminearum* infection, which stimulates the secondary nitrogen responder FgAreA to enter in the nucleus. Subsequently, FgAreA binds to the promoters of DON biosynthesis genes (*FgTRIs*) to rearrange the nucleosome array. The exposure of nucleosome-free regions facilitates FgBre1 binding to *FgTRIs* promoters via its specific basic region leucine zipper (bZIP) domain, thus resulting in the generation of H2B ub1. Further, FgRad6 and FgBre1 recruit FgBre2 to interact with methyltransferase FgSet1 in the COMPASS complex, which enhances the biogenesis of H3K4 me2/3. The enrichment of H2B ub1 and H3K4 me2/3 is necessary for the activation of *FgTRIs* transcription and DON biosynthesis. The blunt-ended arrow in the closed chromatin structure indicates transcriptional inactivation without putrescine induction.

was independent of the presence of FgRad6 and FgBre1 (Figs 7c, S8d). Taken together, these results indicate that FgRad6 and FgBre1 regulate the interaction of FgSet1 and FgBre2 via recruitment of FgBre2 to target chromatin.

Discussion

In this study, we revealed the underlying mechanism for the host stress response metabolite putrescine stimulating DON production during *F. graminearum* infection. Putrescine activates transcription factor FgAreA, and the activated FgAreA promotes H2B ub1 and H3K4 me2/3 deposition on the chromatin region of DON biosynthesis genes *FgTRIs*, which leads to increased *FgTRIs* transcription and ultimately elevated DON biosynthesis (Fig. 8). Previous studies have demonstrated that polyamine participates in DON accumulation of *F. graminearum* during infection (Gardiner *et al.*, 2009, 2010; Bonnighausen *et al.*, 2019). Our study elucidates the elaborate regulatory mechanism, and considerably deepens the understanding of DON production during infection. To cope with biotic and abiotic stresses, polyamines are dramatically induced in plants. In response to biotic stresses, polyamines are conjugated with phenolic acids, and the conjugated polyamines induce systemic protection against a wide range of pathogens including *Blumeria graminis*, *Puccinia recondita*, *Pyrenophora avenae* and *Crinipellis perniciosa* (Walters, 2003; Ross *et al.*, 2004; Haggag & Abd-El-Kareem,

2009). In addition, the metabolites of polyamines result in the accumulation of H₂O₂ that serves as a source for reactive oxygen species to defend against pathogen infection (Walters, 2003). However, our study found that putrescine can also induce DON biosynthesis to advance *F. graminearum* virulence during infection of wheat, which provides a novel insight into the dual roles of polyamines in the interaction between plants and pathogenic fungi.

In many fungi, AreA serving as a conserved zinc finger transcription factor is able to bind the consensus DNA sequence 5'-HGATAR-3' and is responsible for utilization of secondary nitrogen sources (Starich *et al.*, 1998; Jawad *et al.*, 2011b). In *Aspergillus nidulans*, AreA was shown to regulate the chromatin rearrangement in the promoters of nitrate assimilation genes and further promote the occupancy of the transcriptional activator NirA and histone H3 acetylation to activate transcription of *NIIA* and *NIAD* during nitrogen metabolite derepression (Berger *et al.*, 2006, 2008). Apart from its role in nitrogen source metabolism, AreA is also involved in the secondary metabolite biosynthesis. For example, in *F. fujikuroi* and *F. verticillioide*s, AreA orthologs modulate the transcription of the gibberellin and fumonisin B1 biosynthetic genes, respectively (Mihlan *et al.*, 2003; Kim & Woloshuk, 2008; Tudzynski, 2014). However, the mechanism by which AreA modulates secondary metabolite biosynthesis has not been characterized. Our study found that FgAreA modulates DON biosynthesis in *F. graminearum*

(Fig. 1h–j), which is consistent with the previous studies (Min *et al.*, 2012; Yu *et al.*, 2014; Hou *et al.*, 2015). Importantly, FgAreA regulates chromatin rearrangement of DON biosynthetic gene promoters by loosening nucleosome occupation (Fig. 5), which is similar to the function of AreA in regulating nitrogen utilization (Berger *et al.*, 2006, 2008). The loosened chromatin then facilitates the rapid accumulation of FgBre1 and the subsequent H2B ub1 biogenesis during transcriptional activation. Therefore, FgAreA function before H2B ub1 is indispensable for target gene transcriptional activation. Pioneer transcription factors are special proteins capable of initiating targeted chromatin opening, enabling histone modifiers, transcription factors and other DNA binding complexes to promote transcriptional activation (Zaret & Carroll, 2011). Based on our current knowledge, we speculate that FgAreA may act as a pioneer transcription factor both in regulating nitrogen utilization and in secondary metabolite biosynthesis in fungi.

AreA has been reported to be the downstream of target of rapamycin (TOR) signaling pathway in fungi (Crespo & Hall, 2002; Inoki *et al.*, 2005; Di Como & Jiang, 2006). In *S. cerevisiae*, AreA homolog Gln3 is dephosphorylated by Tap42-dissociated phosphatase Sit4 when TOR kinase is inactive, then dephosphorylated Gln3 is dissociated from a cytoplasmic anchor protein Ure2 and imported into the nucleus to regulate transcription (Cooper, 2002; Como & Jiang, 2006). Our previous study showed that FgAreA could partially restore tolerance of the Gln3 mutant to rapamycin and paraquat, indicating that AreA is conserved in *F. graminearum* (Yu *et al.*, 2014). Thus we were interested to examine whether FgAreA is downstream of Tap42-dissociated phosphatases. The *F. graminearum* genome contains three Tap42-dissociated phosphatases, FgPP2A, FgSit4 and FgPpg1. Deletion of FgPP2A is lethal, deletion of FgPpg1 caused reduced DON production, and lack of FgSit4 did not alter DON biosynthesis (Yu *et al.*, 2014). Here, the Co-IP assays revealed that FgAreA interacts with both FgPP2A and FgPpg1 (Fig. S9). Moreover, putrescine treatment increased the interaction strength of FgAreA and FgPP2A, rather than that of FgAreA with FgPpg1 (Fig. S9), suggesting that FgPP2A might be responsible for FgAreA dephosphorylation upon putrescine. However, it is difficult to detect the effect of FgPP2A on FgAreA phosphorylation levels and localization change, as FgPP2A is essential. Collectively, we speculated that the TOR signaling pathway might be involved in FgAreA activation during putrescine-induced DON biosynthesis.

In fungi, the clustered arrangement of secondary metabolite genes allows epigenetic modifications to modulate larger genomic regions efficiently in response to environment stresses (Macheleidt *et al.*, 2016; Dubey & Jeon, 2017). This regulatory model is also applicable to DON biosynthesis in *F. graminearum*. In DON-inducing medium TBI, acetyltransferases FgSas3 (acetylating H3K4), FgGcn5 (acetylating H3K9, H3K18 and H3K27) and FgElp3 (acetylating H3K14) are indispensable for the *FgTRIs* expression and DON biosynthesis (Chen *et al.*, 2018; Kong *et al.*, 2018). Meanwhile, the histone deacetyltransferase Hdf1 was also reported to participate in DON production on spikelets (Li *et al.*, 2011). These studies indicate that precise

histone acetylation is crucial for *FgTRIs* expression. In addition, the deletion of H3K4 methyltransferase FgSet1 reduced *FgTRIs* transcription and DON production in another DON-inducing medium, glucose yeast extract peptone (GYEP) (Liu *et al.*, 2015). Here, we report that a new histone modification H2B ub1 manipulates *FgTRIs* expression and DON production (Fig. 2g, h). H2B ub1 is a prerequisite for H3K4 me2/3 and these two modifications synergistically modulate DON biosynthesis upon putrescine treatment in *F. graminearum* (Fig. 6). To our knowledge, it is the first report that two histone modifications together regulate the transcription of secondary metabolite genes in fungi.

In mammals and yeasts, histone modification H2B ub1 is important for cell growth, development, cell cycle progression, DNA damage response or tumorigenesis (Fuchs & Oren, 2014). Besides, H2B ub1 functions mainly through its downstream histone methylations of H3K4 and H3K79 (Kim *et al.*, 2009; Chandrasekharan *et al.*, 2010; Shilatifard, 2012). Our study found that H2B ub1 regulates growth, DON biosynthesis, virulence and sensitivity to cell wall damage and oxidative stresses in *F. graminearum* (Figs 2g, h, 3c–e, S10a, b). Moreover, the H3K4 me2/3 contributed to major functions of H2B ub1 in *F. graminearum*. RNA-Seq assays for Δ FgBre1 and Δ FgSet1 showed that 1247 genes were regulated by both H2B ub1 and H3K4 me2/3 (Fig. S11a). The Kyoto Encyclopedia of Genes and Genomes (KEGG) pathway analysis showed that these 1247 genes are mainly involved in metabolism of arginine and proline, glyoxylate and dicarboxylate, as well as biosynthesis of secondary metabolites, etc. (Fig. S11b). Accordingly, Δ FgSet1 displayed all defects, including those involving fungal growth, DON biosynthesis, virulence and sensitivity to cell wall damage, detected in Δ FgRad6 and Δ FgBre1 (Figs 6c, d, S10a, b). On the other hand, we obtained H3K79 methyltransferase mutant Δ FgDot1 (Figs S4, S10c), and found that H3K79 methylations, as a branch downstream of H2B ub1, were not involved in the earlier-described FgSet1-mediated biological processes in *F. graminearum*, although they did regulate sensitivity to oxidative stress (Fig. S10b). In the budding yeast, H2B ub1 and H3K79 methylations are crucial for repair of DNA double-strand breaks (Zheng *et al.*, 2018). However, mutants Δ FgRad6, Δ FgBre1 and Δ FgDot1 exhibited similar sensitivity to the DNA-damaging agents hydroxyurea (HU) and 4-nitroquinoline 1-oxide (4-NQO) compared with the wild-type (Fig. S10b), suggesting that H2B ub1 combined with H3K79 methylation is not involved in the response to DNA damage in *F. graminearum*. In addition, H2B ub1 only regulates H3K79 me2/3 in *S. cerevisiae* (Chandrasekharan *et al.*, 2010), while H2B simultaneously controls mono-, di- and trimethylations in *F. graminearum* (Fig. S10c). These results indicate that H2B ub1 has species-specific function in eukaryotic organisms.

H2B ub1 is regulated by Rad6 and Bre1 (human RNF20/40), which is highly conserved in eukaryotes (Fuchs & Oren, 2014). Bre1 is reported to interact with an acidic patch of the nucleosome core particle surface, which positions Rad6 directly next to H2B Lys123, thus facilitating its ubiquitination (Gallego *et al.*, 2016). Moreover, H2B ub1 was responsible for the regulation of inducible transcription instead of constitutive transcription (Segala

et al., 2016). But how H2B ub1 is induced and precisely enriched to the target chromosome is poorly understood. Our study identified a specific DNA-binding domain (bZIP) in FgBre1, and further clarified its function in recognizing target *FgTRIs* under putrescine induction (Fig. 3). These findings uncover, for the first time, the mechanism of H2B ub1 in selecting target chromatin in eukaryotes. Interestingly, phylogenetic and functional analyses showed that this bZIP domain is unique in *Fusarium* species, and Bre1 orthologs of other eukaryotes could not restore the defects of the FgBre1 mutant. Therefore, we deduce that the accumulation of H2B ub1 on target chromatin may depend on different factors in other eukaryotic organisms.

In the budding yeast, H2B ub1-dependent H3K4 methylations are catalyzed by the COMPASS complex, which comprises eight subunits: Set1, Bre2 (Cps60), Swd1 (Cps50), Spp1 (Cps40), Swd2 (Cps35), Swd3 (Cps30), Sdc1 (Cps25) and Cps15 (Shilatfard, 2012). Among these components, Swd1, Swd3, Bre2, Sdc1 and Set1, two domains (SET domain and post-SET domain) constitute the catalytic region of COMPASS, which is crucial for H3K4 methylation activity (Jeon *et al.*, 2018; Hsu *et al.*, 2019). COMPASS subunits Swd2 and Spp1 are significant for H3K4 trimethylation (Vitaliano-Prunier *et al.*, 2008; Shilatfard, 2012; Bae *et al.*, 2020), whereas Cps15 has no effect on the H3K4 methylation pattern (Shilatfard, 2012). Consistent with the results from yeast, we also found that FgSet1, FgSwd1, FgSwd3, FgSdc1 and FgBre2 are key components involved in H3K4 me2/3. However, deletion of the other components, FgSwd2 and FgSpp1, did not affect H3K4 me3 (Fig. S7a), and the Cps15 ortholog was not found in *F. graminearum* (Table S3). More recently, six conserved subunits of COMPASS, including MoBre2, MoSpp1, MoSwd2, MoSdc1, MoSet1 and MoRbBP5 (Cps50), have been identified in *Magnaporthe oryzae* (Zhou *et al.*, 2021). MoSet1 is responsible for methylating H3K4, and MoBre2, MoSwd2 and MoSpp1 are all involved in regulating the H3K4 me3 level, which is also different from the findings in *F. graminearum* (Zhou *et al.*, 2021).

Although H2B ub1 and its downstream H3K4 me2/3 are conserved from yeast to plant and animals, the mechanism for this crosstalk remains controversial and unclear (Jeon *et al.*, 2018; Hsu *et al.*, 2019; Bae *et al.*, 2020). Several regulation models have been proposed in *S. cerevisiae*: H2B ub1 mediates the recruitment of Swd2 to target chromatin, thus facilitating the occurrence of H3K4 me3 (Lee *et al.*, 2007); Rad6 and Bre1 ubiquitylate Swd2 at lysine 68 and 69, and then the ubiquitylated Swd2 regulates H3K4 me3 by recruiting Spp1 to target chromatin (Vitaliano-Prunier *et al.*, 2008); and H2B ub1-induced allosteric rearrangements in the catalytic region of the COMPASS complex render its methylation activity for nucleosomal H3K4 me3 (Jeon *et al.*, 2018; Hsu *et al.*, 2019). Different from the first two models, in which Swd2 plays a key role in H3K4 me3 biogenesis regulated by H2B ub1, we found that FgSwd2 has no effect on H3K4 me2/3 regulation in *F. graminearum*. Interestingly, our study showed that FgRad6 and FgBre1 regulate the interaction of FgBre2 and FgSet1 by recruiting FgBre2 to targeted chromatin regions (Fig. 7c), which may alter the catalytic properties of the COMPASS catalytic component. This case is similar to the third

model mentioned earlier. Studies in *S. cerevisiae* proposed that recognition or sensing of H2B ub1 may trigger allosteric changes in the COMPASS complex catalytic region, which in turn facilitates subsequent nucleosomal H3K4 methylation (Jeon *et al.*, 2018). More recently, cryoelectron microscopy analysis demonstrated that H2B ub1 overrides the inhibitory effect of the Set1 ARM helix by allosterically modulating the packing of the Set1 catalytic domain against Swd1, Bre2 and Swd3 (Hsu *et al.*, 2019), which supports our deduction. To explore the molecular events between H2B ub1 and H3K4 me2/3 in *F. graminearum* precisely, further allosteric study is needed to determine whether the catalytic property of the COMPASS complex is affected by the interaction of FgBre2 and FgSet1.

In conclusion, this study reveals that the transcription factor FgAreA enhances DON production through regulation of H2B ub1 and H3K4 me2/3 enrichment on *FgTRIs* in *F. graminearum* upon exposure to the host defensive compound putrescine during infection. FgAreA-mediated chromatin rearrangement facilitates E3 ligase FgBre1 binding to *FgTRIs*, further promoting H2B ub1 biogenesis under putrescine. Unexpectedly, FgBre1 contains a specific DNA-binding domain, which possesses an ability to recognize target *FgTRIs* genes directly. H2B ub1 accelerates H3K4 me2/3 through strengthening the interaction of FgBre2 and FgSet1 in the presence of putrescine.


Acknowledgements


This research was supported by the National Key R&D Program of China (2018YFE0206000), the Key Project of the National Natural Science Foundation of China (31930088), the National Science Foundation (31871910 and 32072449), the China Agriculture Research System (CARS-3-1-29), the Fundamental Research Funds for the Central Universities 2021FZZX001-31 and the Agriculture and Food Research Initiative of the National Institute of Food and Agriculture, United States Department of Agriculture (award 2018-67013-2851). We thank Prof. Jianhua Huang (Zhejiang University) for providing the *Drosophila melanogaster* cDNA. The authors declare no competing financial interests.


Author contributions

TM conducted most of the experiments; TM and YY designed most of the experiments and directed the project; LZ and YL performed the protein–protein interaction work; MW and YJ performed the ChIP–qPCR analyses; and TM, YY, LW, HCK and ZM analyzed the data and wrote the paper.


ORCID

Harold Corby Kistler  <https://orcid.org/0000-0001-5312-6297>

Tianling Ma  <https://orcid.org/0000-0002-6926-478X>

Zhonghua Ma  <https://orcid.org/0000-0002-5426-0997>

Liang Wu  <https://orcid.org/0000-0003-4953-7258>

Yanni Yin  <https://orcid.org/0000-0002-0798-3420>

Data availability

All the RNA-Seq Illumina data have been deposited at NCBI under the BioProject accession no. PRJNA732727.

References

- Alexander NJ, Proctor RH, McCormick SP. 2009. Genes, gene clusters, and biosynthesis of trichothecenes and fumonisins in *Fusarium*. *Toxin Reviews* 28: 198–215.
- Bae HJ, Dubarry M, Jeon J, Soares LM, Dargemont C, Kim J, Geli V, Buratowski S. 2020. The Set1 N-terminal domain and Swd2 interact with RNA polymerase II CTD to recruit COMPASS. *Nature Communications* 11: 2181.
- Bai GH, Desjardins AE, Plattner RD. 2002. Deoxynivalenol-nonproducing *Fusarium graminearum* causes initial infection, but does not cause disease spread in wheat spikes. *Mycopathologia* 153: 91.
- Beresova A, Renak D, Solcova K, Duplakova N, Honys D. 2009. Functional characterization of bZIP transcription factor in Arabidopsis pollen. *Plant Biology (Rockville)* 2009: 343.
- Berger H, Basheer A, Böck S, Reyes-Dominguez Y, Dalik T, Altmann F, Strauss J. 2008. Dissecting individual steps of nitrogen transcription factor cooperation in the *Aspergillus nidulans* nitrate cluster. *Molecular Microbiology* 69: 1385–1398.
- Berger H, Pachlinger R, Morozov I, Goller S, Narendja F, Caddick M, Strauss J. 2006. The GATA factor AreA regulates localization and *in vivo* binding site occupancy of the nitrate activator NirA. *Molecular Microbiology* 59: 433–446.
- Bonnighausen J, Schauer N, Schafer W, Bormann J. 2019. Metabolic profiling of wheat rachis node infection by *Fusarium graminearum*-decoding deoxynivalenol-dependent susceptibility. *New Phytologist* 221: 459–469.
- Cao F, Chen Y, Cierpicki T, Liu Y, Basrur V, Lei M, Dou Y. 2010. An Ash2L/RbBP5 heterodimer stimulates the MLL1 methyltransferase activity through coordinated substrate interactions with the MLL1 SET domain. *PLoS ONE* 5: e14102.
- Carin J, Diter VW, Wilhelm SF, Karl-Heinz K, Angelika F, Frank JM. 2005. Infection patterns in barley and wheat spikes inoculated with wild-type and trichodiene synthase gene disrupted *Fusarium graminearum*. *Proceedings of the National Academy of Sciences, USA* 102: 16892–16897.
- Chandrasekharan MB, Huang F, Sun Z. 2010. Histone H2B ubiquitination and beyond regulation of nucleosome stability, chromatin dynamics and the trans-histone H3 methylation. *Epigenetics* 5: 460–468.
- Chen Y, Kistler HC, Ma Z. 2019. *Fusarium graminearum* trichothecene mycotoxins: biosynthesis, regulation, and management. *Annual Review of Phytopathology* 57: 15–39.
- Chen Y, Wang J, Yang N, Wen Z, Sun X, Chai Y, Ma Z. 2018. Wheat microbiome bacteria can reduce virulence of a plant pathogenic fungus by altering histone acetylation. *Nature Communications* 9: 3429.
- Cooper TG. 2002. Transmitting the signal of excess nitrogen in *Saccharomyces cerevisiae* from the Tor proteins to the GATA factors: connecting the dots. *FEMS Microbiology Reviews* 26: 223–238.
- Crespo JL, Hall MN. 2002. Elucidating TOR signaling and rapamycin action: lessons from *Saccharomyces cerevisiae*. *Microbiology and Molecular Biology Reviews* 66: 579.
- Crespo-Sempere A, Estiarte N, Marín S, Sanchis V, Ramos AJ. 2015. Targeting *Fusarium graminearum* control via polyamine enzyme inhibitors and polyamine analogs. *Food Microbiology* 49: 95–103.
- Cynthia JK, Peifen Z, Lukas AM, Alfred W, Suzanne P, Martha A, John P, Seung YR, Peter DK. 2004. MetaCyc: a multiorganism database of metabolic pathways and enzymes. *Nucleic Acids Research* 32: 438–442.
- Di Como CJ, Jiang Y. 2006. The association of Tap42 phosphatase complexes with TORC1 – another level of regulation in tor signaling. *Cell Cycle* 5: 2729–2732.
- Dubey A, Jeon J. 2017. Epigenetic regulation of development and pathogenesis in fungal plant pathogens. *Molecular Plant Pathology* 18: 887–898.
- Feng J, Akira K, Takashi N. 2008. Effects of different carbon sources on trichothecene production and *Tri* gene expression by *Fusarium graminearum* in liquid culture. *FEMS Microbiology Letters* 285: 212–219.
- Fuchs G, Oren M. 2014. Writing and reading H2B monoubiquitylation. *Biochimica et Biophysica Acta (BBA) – Gene Regulatory Mechanisms* 1839: 694–701.
- Gallego LD, Ghodgaonkar Steger M, Polyansky AA, Schubert T, Zagrovic B, Zheng N, Clausen T, Herzog F, Köhler A. 2016. Structural mechanism for the recognition and ubiquitination of a single nucleosome residue by Rad6–Bre1. *Proceedings of the National Academy of Sciences, USA* 113: 10553–10558.
- Gardiner DM, Kazan K, Manners JM. 2009. Nutrient profiling reveals potent inducers of trichothecene biosynthesis in *Fusarium graminearum*. *Fungal Genetics and Biology* 46: 604–613.
- Gardiner DM, Kazan K, Praud S, Torney FJ, Rusu A, Manners JM. 2010. Early activation of wheat polyamine biosynthesis during *Fusarium* head blight implicates putrescine as an inducer of trichothecene mycotoxin production. *BMC Plant Biology* 10: 289.
- Goswami RS, Kistler HC. 2004. Heading for disaster: *Fusarium graminearum* on cereal crops. *Molecular Plant Pathology* 5: 515–525.
- Haggag WM, Abd-El-Kareem F. 2009. Methyl jasmonate stimulates polyamines biosynthesis and resistance against leaf rust in wheat plants. *Archives of Phytopathology and Plant Protection* 42: 16–31.
- Hou R, Jiang C, Zheng Q, Wang C, Xu J. 2015. The AreA transcription factor mediates the regulation of deoxynivalenol (DON) synthesis by ammonium and cyclic adenosine monophosphate (cAMP) signalling in *Fusarium graminearum*. *Molecular Plant Pathology* 16: 987–999.
- Hsu PL, Shi H, Leonen C, Kang J, Chatterjee C, Zheng N. 2019. Structural basis of H2B ubiquitination-dependent H3K4 methylation by COMPASS. *Molecular Cell* 76: 712–723.
- Ilgel P, Hadelar B, Maier FJ, Schaefer W. 2009. Developing kernel and rachis node induce the trichothecene pathway of *Fusarium graminearum* during wheat head infection. *Molecular Plant-Microbe Interactions* 22: 899–908.
- Inoki K, Ouyang H, Li Y, Guan KL. 2005. Signaling by target of rapamycin proteins in cell growth control. *Microbiology and Molecular Biology Reviews* 69: 79.
- Jawad M, Florence R, Christian B. 2011a. The pH regulatory factor Pac1 regulates *Tri* gene expression and trichothecene production in *Fusarium graminearum*. *Fungal Genetics and Biology* 48: 275–284.
- Jawad M, Florence R, Christian B. 2011b. Regulation of trichothecene biosynthesis in *Fusarium*: recent advances and new insights. *Applied Microbiology and Biotechnology* 91: 519–528.
- Jeon J, McGinty RK, Muir TW, Kim J, Kim J. 2018. Crosstalk among Set1 complex subunits involved in H2B ubiquitylation-dependent H3K4 methylation. *Nucleic Acids Research* 46: 11129–11143.
- Kaster M, Laubinger S. 2016. Determining nucleosome position at individual loci after biotic stress using MNase-qPCR. *Environmental Responses in Plants* 1398: 357–372.
- Kaufmann K, Mui OJM, Ster SM, Farinelli L, Krajewski P, Angenent GC. 2010. Chromatin immunoprecipitation (ChIP) of plant transcription factors followed by sequencing (ChIP-SEQ) or hybridization to whole genome arrays (ChIP-CHIP). *Nature Protocols* 5: 457.
- Kazan K, Gardiner DM, Manners JM. 2012. On the trail of a cereal killer: recent advances in *Fusarium graminearum* pathogenomics and host resistance. *Molecular Plant Pathology* 13: 399–413.
- Kim H, Lee S, Jo S, McCormick SP, Butchko RAE, Proctor RH, Yun S. 2013. Functional roles of FgLaEa in controlling secondary metabolism, sexual development, and virulence in *Fusarium graminearum*. *PLoS ONE* 8: e684417.
- Kim H, Woloshuk CP. 2008. Role of AREA, a regulator of nitrogen metabolism, during colonization of maize kernels and fumonisin biosynthesis in *Fusarium verticillioides*. *Fungal Genetics and Biology* 45: 947–953.
- Kim J, Guermah M, McGinty RK, Lee J, Tang Z, Milne TA, Shilatifard A, Muir TW, Roeder RG. 2009. RAD6-mediated transcription-coupled H2B ubiquitylation directly stimulates H3K4 methylation in human cells. *Cell* 137: 459–471.
- Kong X, van Diepeningen AD, van der Lee TAJ, Waalwijk C, Xu J, Xu J, Zhang H, Chen W, Feng J. 2018. The *Fusarium graminearum* histone

- acetyltransferases are important for morphogenesis, DON biosynthesis, and pathogenicity. *Frontiers in Microbiology* 9: 654.
- Kruger AN, Brogley MA, Huizinga JL, Kidd JM, de Rooij DG, Hu Y, Mueller JL. 2019. A neofunctionalized X-linked ampliconic gene family is essential for male fertility and equal sex ratio in mice. *Current Biology* 29: 3699.
- Lee HJ, Ryu D. 2017. Worldwide occurrence of mycotoxins in cereals and cereal-derived food products: public health perspectives of their co-occurrence. *Journal of Agricultural and Food Chemistry* 65: 7034–7051.
- Lee JS, Shukla A, Schneider J, Swanson SK, Washburn MP, Florens L, Bhaumik SR, Shilatifard A. 2007. Histone crosstalk between H2B monoubiquitination and H3 methylation mediated by COMPASS. *Cell* 131: 1084–1096.
- Li Y, Wang C, Liu W, Wang G, Kang Z, Kistler HC, Xu J. 2011. The HDF1 histone deacetylase gene is important for conidiation, sexual reproduction, and pathogenesis in *Fusarium graminearum*. *Molecular Plant-Microbe Interactions* 24: 487–496.
- Liu Y, Liu N, Yin Y, Chen Y, Jiang J, Ma Z. 2015. Histone H3K4 methylation regulates hyphal growth, secondary metabolism and multiple stress responses in *Fusarium graminearum*. *Environmental Microbiology* 17: 4615–4630.
- Liu Y, Lu Y, Wang L, Chang F, Yang L. 2016. Occurrence of deoxynivalenol in wheat, Hebei Province, China. *Food Chemistry* 197: 1271–1274.
- Ma L, Li CZ. 2010. Effects of cobalt and DFMA on polyamine content and membrane-lipid peroxidation in wheat seedling under osmotic stresses. *Agricultural Research in the Arid Areas* 28: 136.
- Macheleidt J, Mattern DJ, Fischer J, Netzker T, Weber J, Schroeckh V, Valiante V, Brakhage AA. 2016. Regulation and role of fungal secondary metabolites. *Annual Review of Genetics* 50: 371–392.
- Matam P, Parvatam G. 2017. Putrescine and polyamine inhibitors in culture medium alter in vitro rooting response of *Decalepis hamiltonii* Wight & Arn. *Plant Cell Tissue and Organ Culture (PCTOC)* 128: 273–282.
- Merhej J, Boutigny AL, Pinson-Gadais L, Richard-Forget F, Barreau C. 2010. Acidic pH as a determinant of *TRI* gene expression and trichothecene B biosynthesis in *Fusarium graminearum*. *Food Additives and Contaminants Part A-Chemistry Analysis Control Exposure & Risk Assessment* 27: 710–717.
- Merhej J, Urban M, Dufresne M, Hammond-Kosack KE, Richard-Forget F, Barreau C. 2012. The velvet gene, *FgVe1*, affects fungal development and positively regulates trichothecene biosynthesis and pathogenicity in *Fusarium graminearum*. *Molecular Plant Pathology* 13: 363–374.
- Mihlan M, Homann V, Liu T, Tudzynski B. 2003. AREA directly mediates nitrogen regulation of gibberellin biosynthesis in *Gibberella fujikuroi*, but its activity is not affected by NMR. *Molecular Microbiology* 47: 975–991.
- Min K, Shin Y, Son H, Lee J, Kim JC, Choi GJ, Lee YW. 2012. Functional analyses of the nitrogen regulatory gene *areA* in *Gibberella zeae*. *FEMS Microbiology Letters* 334: 66–73.
- Mudge AM, Dill-Macky R, Dong Y, Gardiner DM, White RG, Manners JM. 2006. A role for the mycotoxin deoxynivalenol in stem colonisation during crown rot disease of wheat caused by *Fusarium graminearum* and *Fusarium pseudograminearum*. *Physiological and Molecular Plant Pathology* 69: 73–85.
- Nadia P, Laetitia PG, Anne-Laure B, Christian B, Florence RF. 2011. Cinnamic-derived acids significantly affect *Fusarium graminearum* growth and in vitro synthesis of type B trichothecenes. *Phytopathology* 101: 929–934.
- Pestka JJ. 2010. Deoxynivalenol: mechanisms of action, human exposure, and toxicological relevance. *Archives of Toxicology* 84: 663–679.
- Ponts N, Pinson-Gadais L, Barreau C, Richard-Forget F, Ouellet T. 2007. Exogenous H₂O₂ and catalase treatments interfere with *Tri* genes expression in liquid cultures of *Fusarium graminearum*. *FEBS Letters* 581: 443–447.
- Ross WF, Walters DR, Robins DJ. 2004. Synthesis and antifungal activity of five classes of diamines. *Pest Management Science* 60: 143–148.
- Segala G, Benness MA, Pandey DP, Hulo N, Picard D. 2016. Monoubiquitination of histone H2B blocks eviction of histone variant H2A.z from inducible enhancers. *Molecular Cell* 64: 334–346.
- Shilatifard A. 2012. The COMPASS family of histone H3K4 methylases: mechanisms of regulation in development and disease pathogenesis. *Annual Review of Biochemistry* 81: 65–95.
- Sood V, Cajigas I, D'Urso A, Light WH, Brickner JH. 2017. Epigenetic transcriptional memory of *GAL* genes depends on growth in glucose and the Tup1 transcription factor in *Saccharomyces cerevisiae*. *Genetics* 206: 1895–1907.
- Starich MR, Wikstrom M, Arst HN, Clore GM, Gronenborn AM. 1998. The solution structure of a fungal AREA protein-DNA complex: an alternative binding mode for the basic carboxyl tail of GATA factors. *Journal of Molecular Biology* 277: 605–620.
- Stephens AE, Gardiner DM, White RG, Munn AL, Manners JM. 2008. Phases of infection and gene expression of *Fusarium graminearum* during crown rot disease of wheat. *Molecular Plant-Microbe Interactions* 21: 1571–1581.
- Tudzynski B. 2014. Nitrogen regulation of fungal secondary metabolism in fungi. *Frontiers in Microbiology* 5: 656.
- Vitaliano-Prunier A, Menant A, Hobeika M, Géli V, Gwizdek C, Dargemont C. 2008. Ubiquitylation of the COMPASS component Swd2 links H2B ubiquitylation to H3K4 trimethylation. *Nature Cell Biology* 10: 1365–1371.
- Voigt CA, Schafer W, Salomon S. 2005. A secreted lipase of *Fusarium graminearum* is a virulence factor required for infection of cereals. *The Plant Journal* 42: 364–375.
- Walters D. 2003. Resistance to plant pathogens: possible roles for free polyamines and polyamine catabolism. *New Phytologist* 159: 109–115.
- Wood A, Krogan NJ, Dover J, Schneider J, Heidt J, Boateng MA, Dean K, Golshani A, Zhang Y, Greenblatt JF et al. 2003. Bre1, an e3 ubiquitin ligase required for recruitment and substrate selection of rad6 at a promoter. *Molecular Cell* 11: 267–274.
- Woodworth AM, Holloway AF. 2016. The role of epigenetic regulation in transcriptional memory in the immune system. *Advances in Protein Chemistry & Structural Biology* 106: 43–69.
- Yamamoto A, Shim IS, Fujihara S. 2017. Inhibition of putrescine biosynthesis enhanced salt stress sensitivity and decreased spermidine content in rice seedlings. *Biologia Plantarum* 61: 385–388.
- Yu F, Gu Q, Yun Y, Yin Y, Xu JR, Shim WB, Ma Z. 2014. The TOR signaling pathway regulates vegetative development and virulence in *Fusarium graminearum*. *New Phytologist* 203: 219–232.
- Yun Y, Liu Z, Yin Y, Jiang J, Yun C, Xu J, Ma Z. 2015. Functional analysis of the *Fusarium graminearum* phosphatome. *New Phytologist* 207: 119–134.
- Zaret KS, Carroll JS. 2011. Pioneer transcription factors: establishing competence for gene expression. *Genes & Development* 25: 2227–2241.
- Zheng S, Li D, Lu Z, Liu G, Wang M, Xing P, Wang M, Dong Y, Wang X, Li J et al. 2018. Bre1-dependent H2B ubiquitination promotes homologous recombination by stimulating histone eviction at DNA breaks. *Nucleic Acids Research* 46: 11326–11339.
- Zhou S, Liu X, Sun W, Zhang M, Wang W. 2021. The COMPASS-like complex modulates fungal development and pathogenesis by regulating H3K4me3-mediated targeted gene expression in *Magnaporthe oryzae*. *Molecular Plant Pathology* 22: 422–439.

Supporting Information

Additional Supporting Information may be found online in the Supporting Information section at the end of the article.

Fig. S1 Endogenous putrescine synthesis-encoding gene *FgODC* is not upregulated during *F. graminearum* infection on wheat.

Fig. S2 DON-inducing carbon source could not activate transcription factor *FgAreA*.

Fig. S3 The transcription level and protein abundance of *FgAreA* were not altered upon putrescine treatment.

Fig. S4 Construction and identification of *FgRAD6*, *FgBRE1* and *FgDOT1* gene deletion mutants.

Fig. S5 Phylogenetic analysis of Rad6 orthologs from *F. graminearum* and other eukaryotic organisms.

Fig. S6 Global H3K4 me levels were not changed upon putrescine treatment.

Fig. S7 H3K4 methyltransferase complex COMPASS is crucial for DON production and *FgTRIs* transcription.

Fig. S8 Function analysis of the interaction between FgRad6/FgBre1 and FgBre2/FgSet1.

Fig. S9 FgAreA interacts with both FgPP2A and FgPpg1, and putrescine increases the interaction strength between FgAreA and FgPP2A.

Fig. S10 H2B ub1 regulates growth, virulence and sensitivity to stresses via its downstream H3K4 and H3K79 methylations.

Fig. S11 H2B ub1 and H3K4 me2/3 coregulate multiple biological processes in *F. graminearum*.

Methods S1 Supplementary materials and methods.

Table S1 Primers used in this study and their relevant characteristics.

Table S2 A list of FgAreA-interacting proteins identified by affinity capture in coupling with MS.

Table S3 Putative COMPASS subunits were identified by BLASTP analysis.

Please note: Wiley Blackwell are not responsible for the content or functionality of any Supporting Information supplied by the authors. Any queries (other than missing material) should be directed to the *New Phytologist* Central Office.